

ISSN 8755-6839

SCIENCE OF TSUNAMI HAZARDS

The International Journal of The Tsunami Society
Volume 29 Number 1 Published Electronically 2010

SATELLITE TRANSMITTED FLOOD ALERTS TO REDUCE FATALITIES AND INJURIES ON THE ISLAND OF HAWAII ASSOCIATED WITH LOCALLY GENERATED TSUNAMIS 1

Daniel A. Walker - *Storm and Tsunami Flood Gauges, Haleiwa, Hawaii, USA*

DESIGN LOAD EVALUATION FOR TSUNAMI SHELTERS BASED ON DAMAGE OBSERVATIONS AFTER INDIAN OCEAN TSUNAMI DISASTER DUE TO THE 2004 SUMATRA EARTHQUAKE 11

Y. Nakano - *Dept. of Fundamental Engineering, Institute of Industrial Science, University of Tokyo, Tokyo, JAPAN*

A STUDY OF THE EDGE WAVE EFFECTS INDUCED BY THE TSUNAMI OF 26 DECEMBER 2004 AT PHI-PHI ISLAND IN THAILAND 21

R.H.C. Wong - *Dept. Civil & Structural Engineering, Hong Kong Polytechnic Univ., Hong Kong, CHINA*

H.Y. Lin - *Dept. Civil & Structural Engineering, Hong Kong Polytechnic Univ., Hong Kong, CHINA*

K.T. Chau - *Dept. Civil & Structural Engineering, Hong Kong Polytechnic Univ., Hong Kong, CHINA*

O.W.H. Wai - *Dept. Civil & Structural Engineering, Hong Kong Polytechnic Univ., Hong Kong, CHINA*

DETERMINISTIC ANALYSIS OF THE TSUNAMI HAZARD IN CHINA 32

Yefei Ren - *Dept. of Information Technology and Engineering Material, Institute of Engineering Mechanics, Harbin. CHINA.*

Ruizhi Wen - *Dept. of Information Technology and Engineering Material, Institute of Engineering Mechanics, Harbin. CHINA*

Baofeng Zhou - *Dept. of Information Technology and Engineering Material, Institute of Engineering Mechanics, Harbin. CHINA*

TSUNAMI SOCIETY INTERNATIONAL, 1741 Ala Moana Blvd. #70, Honolulu, HI 96815, USA.

WWW.TSUNAMISOCIETY.ORG

SCIENCE OF TSUNAMI HAZARDS is a CERTIFIED OPEN ACCESS Journal included in the prestigious international academic journal database DOAJ maintained by the University of Lund in Sweden with the support of the European Union. 'SCIENCE OF TSUNAMI HAZARDS is also preserved and archived at the National Library, The Hague, NETHERLANDS, at the Library of Congress, Washington D.C., USA, and in the Electronic Library of Los Alamos, National Laboratory, New Mexico, USA.

OBJECTIVE: The Tsunami Society publishes this journal to increase and disseminate knowledge about tsunamis and their hazards.

DISCLAIMER: Although these articles have been technically reviewed by peers, the Tsunami Society is not responsible for the veracity of any statement, opinion or consequences.

EDITORIAL STAFF

Dr. George Pararas-Carayannis, Editor
1741 Ala Moana Blvd. No 70, Honolulu, Hawaii 96815, USA. <mailto:drgeorgepc@yahoo.com>

EDITORIAL BOARD

Dr. Charles MADER, Mader Consulting Co., Colorado, New Mexico, Hawaii, USA
Dr. Hermann FRITZ, Georgia Institute of Technology, USA
Prof. George CURTIS, University of Hawaii -Hilo, USA
Dr. Tad S. MURTY, University of Ottawa, CANADA
Dr. Zygmunt KOWALIK, University of Alaska, USA
Dr. Galen GISLER, NORWAY
Prof. Kam Tim CHAU, Hong Kong Polytechnic University, HONG KONG
Dr. Jochen BUNDSCHUH, (ICE) COSTA RICA, Royal Institute of Technology, SWEDEN
Dr. Yurii SHOKIN, Novosibirsk, Russian Federation

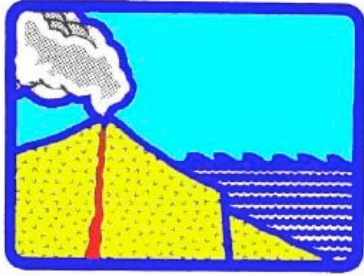
TSUNAMI SOCIETY OFFICERS

Dr. George Pararas-Carayannis, President; Dr. Tad Murty, Vice President; Dr. Carolyn Forbes, Secretary/Treasurer.

Submit manuscripts of articles, notes or letters to the Editor. If an article is accepted for publication the author(s) must submit a scan ready manuscript, a Doc, TeX or a PDF file in the journal format. Issues of the journal are published electronically in PDF format. Recent journal issues are available at: <http://www.TsunamiSociety.org>

Tsunami Society members will be advised by e-mail when a new issue is available. There are no page charges for one paper per calendar year for authors who are members of Tsunami Society International. Permission to use figures, tables and brief excerpts from this journal in scientific and educational works is hereby granted provided that the source is acknowledged.

Issues of the journal (ISSN 8755-6839) from 1982 thru 2005 are available in PDF format at <http://epubs.lanl.gov/tsunami/> and at WWW.TSUNAMISOCIETY.ORG or on a CD-ROM that may be purchased by contacting Tsunami Society International at tsunamisociety@hawaiiantel.net



SCIENCE OF TSUNAMI HAZARDS

International Journal of the Tsunami Society

Volume 29

Number 1

2010

SATELLITE TRANSMITTED FLOOD ALERTS TO REDUCE FATALITIES AND INJURIES ON THE ISLAND OF HAWAII ASSOCIATED WITH LOCALLY GENERATED TSUNAMIS

Daniel A. Walker

Storm and Tsunami Flood Gauges

59-530 Pupukea Rd.

Haleiwa, HI 96712, USA

ABSTRACT

Tsunami detection instruments were installed along remote shoreline campgrounds of Hawaii Volcanoes National Park in August of 2009. Components include water sensing devices at elevations of about 10 feet above sea level located at distances of about 200 feet from the shoreline and satellite communicators located further inland at higher elevations that will send daily status reports and flood alerts from the water sensors as they occur to the Pacific Tsunami Warning Center in Honolulu. Such instruments will provide for earlier warnings of significant locally generated tsunamis than previously possible. These instruments will also provide a basis for early warnings of locally generated tsunamis to those campgrounds using siren systems to be designed specifically for those remote environments. Suggestions of additional actions that could also reduce future fatalities and injuries at those campgrounds as a result of locally generated tsunamis are also provided in this report.

1. INTRODUCTION

Data for all of the reported significant locally generated tsunamis in the Hawaiian Islands during the 20th century are shown in Figures 1 and 2. A significant tsunami is considered here to be a tsunami with a runup of three or more feet. Runup is a measure of the tsunami's maximum vertical wave height on land relative to mean sea level. Inundation is a measure of the tsunami's maximum horizontal inland penetration. Also shown are data for the largest known and best documented local tsunami of the 19th century in Figure 3. No significant locally generated tsunamis have occurred in the Hawaiian Islands thus far in the 21st century and there are no reports of any local tsunamis having significant runups on any island other than the Big Island.

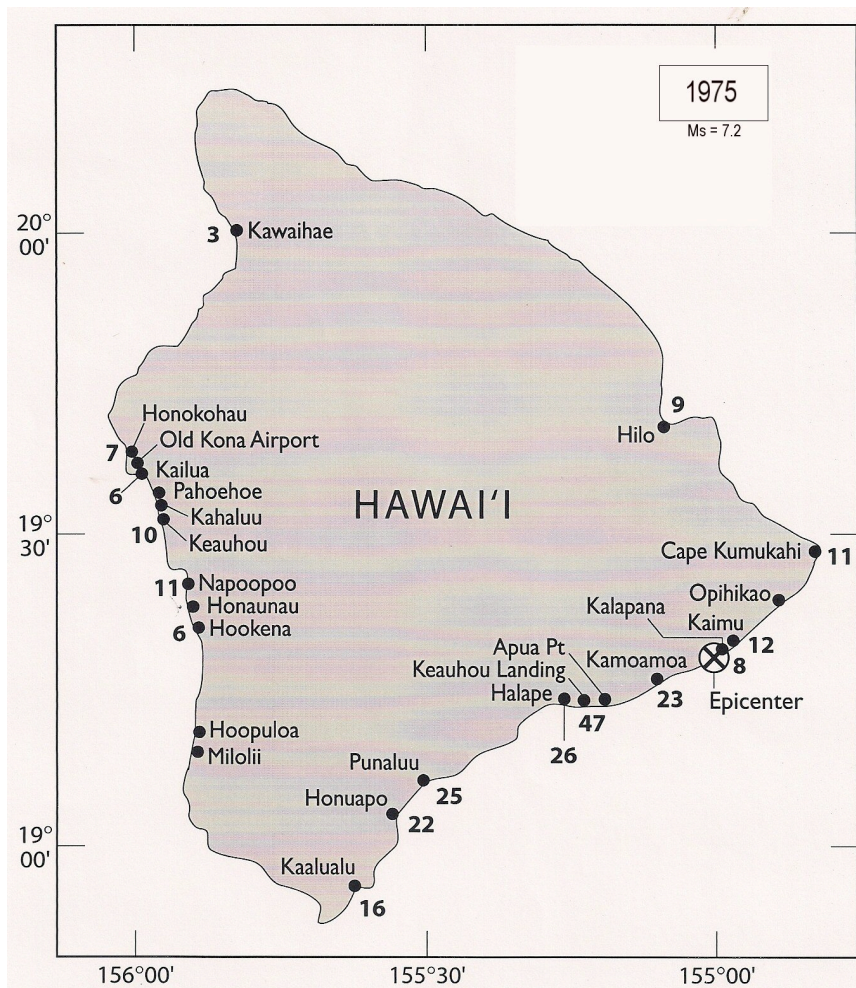


Figure 1. Earthquake epicenter, magnitude, and run-up values in feet for the 1975 tsunami (Lander and Lockridge, 1989). Run-ups are generally maximum vertical measurements of a tsunami's wave height relative to mean sea level. Inundation is a measure of a tsunami's maximum horizontal inland penetration.

Note that some tsunamis (Figure 2) have occurred as a result of relatively small or unfelt earthquakes. Also, another possible unfelt earthquake generating a tsunami is one that may have occurred in 1869 with a run-up of about 27 feet between Pohoiki and Opihikao and inundation of about 800 feet (Cox and Morgan, 1977; and personal communication). Of the 23 Big Island earthquakes in the 20th century (Klein et al. 2001) with magnitudes of 6.0 or greater plus the 15 October 2006 earthquake near Kiholo, only the three shown in Figures 1 and 2 generated significant tsunamis. All of the foregoing data indicates that earthquake magnitudes are not reliable indicators of tsunamigenic potential. A better indicator would be actual evidence of a tsunami washing inland soon after the recording of a nearby earthquake.

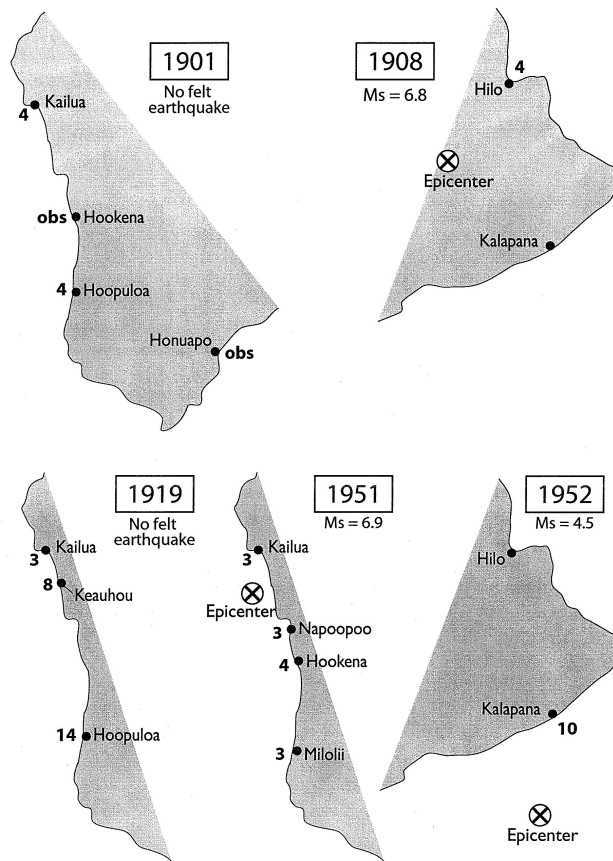


Figure 2. Earthquake epicenters, magnitudes, and run-up values in feet for other significant local tsunamis in the 20th century (Lander and Lockridge, 1989). In Hawaii newspaper articles discussing the 1901 and 1919 tsunamis, there were no reports of any felt earthquakes that might be associated with these tsunamis. There were also no reports of any instrumentally recorded earthquakes by the Hawaiian Volcano Observatory, which was in operation at the time of the 1919 tsunami. The 1901 tsunami was reported to have moved progressively southward from Kailua and around to Honuapo.

To provide such information water sensing and transmitting devices (cellular runup detectors or CRD's) were built and placed on Civil Defense siren poles at Punaluu, Honuapo, Milolii, Honaunau,

Napoopoo, Kahaluu, Pahoeohoe Park, and the old Kona airport (Figure 4; Walker and Cessaro, 2002). Although these instruments complement the Pacific Tsunami Warning Center's (PTWC) sea level gauges at Kapoho, Honuapo, Milolii, and Honokohau, neither CRD's nor sea level gauges exist in the highly seismically active region of the Big Island extending from Punaluu to PTWC's sea level gauge at Kapoho. Much of this region is within the boundaries of Hawaii Volcanoes National Park (HAVO) with no roads, power, or civil defense siren poles. The largest locally generated tsunamis in Hawaii's history occurred in this region (Figures 1 and 3). Therefore tsunami detection instruments in these areas could provide for earlier, life saving warnings for heavily used parks to the north (Pohoiki and Ahalanui) and south (Punaluu and Honuapo). Also, much earlier warnings for the Hilo area and the Kona coast would be possible.

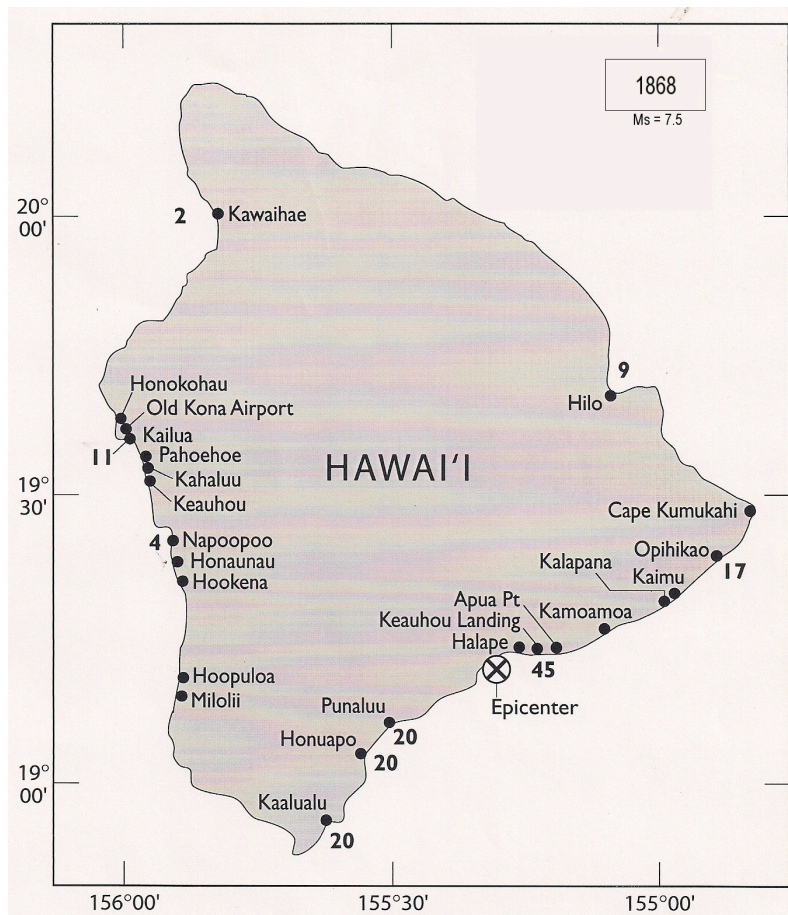


Figure 3. Earthquake epicenter, magnitude, and run-up values in feet for the 1868 tsunami (Lander and Lockridge, 1989). In addition, there are reports of the tsunami being observed at other Big Island locations. A value of 7 feet indicated for Apua may not be consistent with reports that all of the houses in the area were washed away. It should be noted that the waves could have been much larger as they swept across this extensive low-lying point of land. There may have been no topographic features in the area capable of providing reliable evidence of higher run-ups.

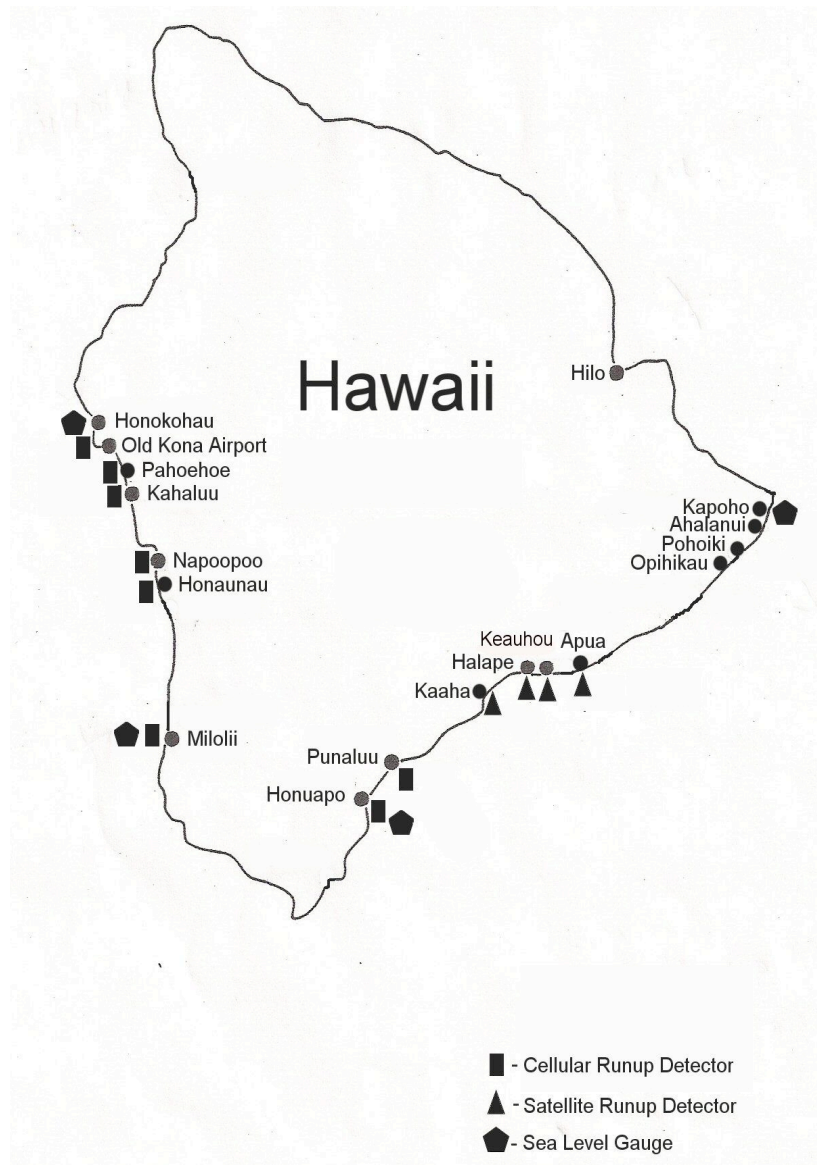


Figure 4. Site locations for Cellular Run-up Detectors (CRD's), Satellite Run-up Detectors (SRD's), and nearby Pacific Tsunami Warning Center sea level gauges.

2. INSTRUMENTATION

Detectors consisting of water sensors and satellite communicators (SRD's) were built and housed in artificial rocks. These units were deployed at the Apua, Keauhou, Halape, and Kaaha campgrounds. The sensors are generally from about 8 to 10 feet above mean sea level and about 125 to 300 feet from the shoreline. The satellite communicators are further inland at higher elevations. Once flooding occurs an email is received at PTWC in about 1 to 2 minutes. If an earthquake occurred in the area

just prior to the email receipt, confirmation of a significant tsunami should be assumed and warnings immediately issued. The instruments have been designed and tested to run on primary lithium batteries for at least one year without maintenance.

Another device that was installed at the Halape site was a “campground siren system”. This device consists of a water sensor and siren, each mounted in an artificial rock. These also have been built and tested to run on primary lithium ion batteries for at least one year without maintenance. However, because of the extensive lateral distribution and the shoreline proximity of the individual campsites at each of the four campgrounds described below, design modifications of the existing “campground siren system” will be required.

Asset: Sixth Unit		Message History (54 Messages)	
AdC Ocean Region	Date (PDT)	Event Report	Location Proximity
2MJA2 PORSG	2009-08-24 15:44:55	Position Report	19.26050,-155.30200 3552.12 mi SW of Monterrey
2MJA2 PORSG	2009-08-23 15:44:55	Position Report	19.26050,-155.30200 3552.12 mi SW of Monterrey
2MJA2 PORSG	2009-08-22 15:44:56	Position Report	19.26067,-155.30183 3552.11 mi SW of Monterrey
2MJA2 PORSG	2009-08-21 15:44:55	Position Report	19.26033,-155.30183 3552.12 mi SW of Monterrey
2MJA2 PORSG	2009-08-20 15:44:55	Position Report	19.26050,-155.30200 3552.12 mi SW of Monterrey
2MJA2 PORSG	2009-08-19 15:44:55	Position Report	19.26050,-155.30200 3552.12 mi SW of Monterrey
2MJA2 PORSG	2009-08-18 15:44:55	Position Report	19.26050,-155.30200 3552.12 mi SW of Monterrey
2MJA2 PORSG	2009-08-17 15:44:55	Position Report	19.26050,-155.30200 3552.12 mi SW of Monterrey

Figure 5. Examples of daily SRD system position reports from 17 through 24 August of 2009 at Kaaha available to authorized subscribers of the satellite service.

3. CAMPSITE ENVIRONMENTS

Halape is about a four to five hour, one-way hike from the nearest road across old lava flows with little or no vegetation. Keauhou and Apua are along the same route. Keauhou is about three to four hours away from the road and Apua is about two to three hours away. Kaaha is about two to three

hours from its nearest road down a steep rubble switchback and across a plateau of lava flows gently sloping towards the ocean.

At all four campgrounds, campers predominantly pitch their tents or sleeping bags on the beach because of the beauty of that environment and because of necessity. These campsites are generally within 100 feet of the shoreline at elevations less than 6 feet above sea level. The sand provides a flat, smooth surface, unlike the irregular rocky surfaces further inland. These individual beach campsites are in some instances spread out over several hundred feet of the shoreline, often under any available cluster of trees, providing ample opportunities for privacy. A single, approximate 12-foot by 12 foot shelter with a smooth dirt floor does exist at each of the Keauhou, Halape, and Kaaha camping areas. At distances of more than a thousand feet from the shoreline and elevations generally more than 50 feet above sea level, these shelters are well located outside of the inundation zone for even the largest tsunamis. If the campers were aware of the detailed history of tsunamis at these sites, some would opt for the shelters, at least for sleeping, rather than the beach. However, with overcrowding (i.e., perhaps as little as more than two tents) the relatively small but safe shelters cannot compete with the numerous private sites at the shorelines.

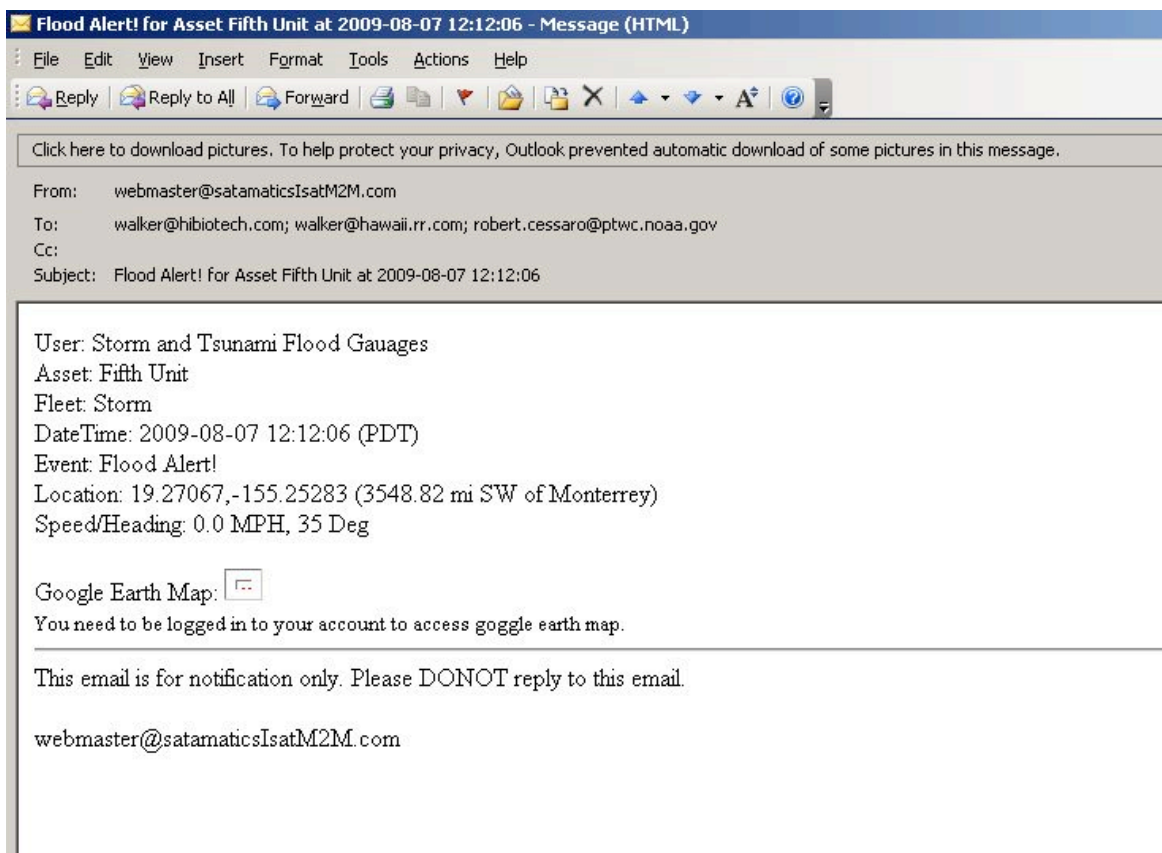


Figure 6. An example of a flood alert sent to authorized subscribers of the satellite service. This alert is for a flood test at Halape on 7 August 2009.

The sensor for the “campground siren system” installed at Halape is only a couple of feet below the elevation of most of the shoreline campsites, so it may, in most instances, provide for warnings of little value. Were the campsites further inland, at higher elevations, and not so widely distributed along the beach, such a system could be more effective. At Apua, Keauhou, and Kaaha there were no locations for which the existing “campground siren system” could serve any useful purpose. It will be important to monitor the survivability of the “campground siren system” and the four SRD systems in terms of heat, rain, insects, rodents, and humans. A unit on Oahu in a cooler, wetter environment with potentially less insect, rodent, or human interaction has thus far (through August 2009) operated without any problems or required battery changes for 10 months, giving daily position reports (Figure 5) and numerous flood alert test messages (Figure 6) during this time period.

4. CONCLUSIONS AND RECOMMENDATIONS

Until more information is gathered on the reliability of the SRD systems in field operations, the absence of a flood alert should not be used as evidence that water did not flood a sensor. However, if a unit has generally been giving daily position reports and a flood alert was received shortly after a nearby earthquake was recorded, a warning should be issued immediately for the Big Island and modified accordingly as other data is received.

Although the systems installed at the shoreline campgrounds will provide earlier and more reliable warnings for areas outside HAVO via civil defense sirens, there is at present no effective way to warn visitors to these campgrounds of impending local or Pacific-wide tsunamis. However, the technology already exists to provide such warnings. The SRD systems now installed at the shoreline campgrounds will provide early evidence of a local tsunami. Each of the four campgrounds has a toilet building in which a powerful siren could be mounted and remotely triggered by Civil Defense or HAVO using the same type of satellite communicator that detected the initial tsunami inundation. Make no mistake – if the earliest detectable landfall of a significant tsunami is at one of HAVO’s shoreline campgrounds there could be fatalities and injuries. This could occur for a felt earthquake if visitors stayed to watch or pick up fish. Or it could occur if they were at the beach and the tsunami was generated by a smaller unfelt earthquake that may have triggered a large submarine landslide. However, campers at adjacent campgrounds might be saved if the initial detected flooding results in sirens being turned on at those other campgrounds before the tsunami strikes.

Additional tsunami detection instruments near the margins of HAVO’s shoreline boundaries further to the north and further to the south could also improve the speed with which warnings could be given at the campgrounds for some local tsunamis if inundation occurs at those more northerly or southerly locations prior to inundations at any of the shoreline campgrounds. Such locations for additional instruments could be critical for more timely warnings for areas to the north (Pohoiki, Ahalanui, and on to Hilo) and to the south (Punaluu, Honuapo, and on to the Kona Coast).

There are risks associated with everyday activities and special risks may be associated with hiking and camping in our national parks. HAVO is no exception. Hikers and campers need to be aware of special risks and reasonable efforts should be taken to reduce such risks. Visitors to shoreline areas need to be advised of the risks posed by tsunamis. Some information is already provided to them when they apply for their backcountry permits. Such information should be accurate, comprehensive, and updated as new equipment is placed in the field or as warning systems evolve. Also, shelters

should be safely located outside of tsunami inundation zones. The existing shelters fulfill this requirement. However, considering environmental and budgetary constraints, as well as other priorities, more safe campsites at Apua, Keauhou, Halape, and Kaaha should be considered. These could consist of nothing more than a couple of roof panels, dirt flooring, and supporting 2 x 4's or 4 x 4's. Such shelters could be used for sleeping at night when campers would be most vulnerable to an unfelt but dangerous local tsunami. These shelters would provide the level flooring that is nearly impossible to find anywhere but near the shoreline and at the single safe inland shelters at Keauhou, Halape, and Kaaha. Adding lean-to's to either side of the existing inland shelters or simple commercially available shelters are another possibility. An extreme minimalist but workable solution could be the mere landscaping of several flat dirt areas scattered sufficiently inland to provide safety and privacy. These "tsunami safe sleeping areas" could be indicated by ahu's (stacked rocks) and their use for safe sleeping should be encouraged. Although many campers may continue to take their chances sleeping at the beach, with sufficient inland campsites, comprehensive information, and adequate warnings given, responsible action would have been taken by HAVO to prevent any tsunami fatalities or injuries.

5. SUMMARY

5.1 Tsunami detection and flood alert satellite transmission instruments have been installed at Apua Point, Keauhou Landing, Halape, and Kaaha capable of providing earlier warnings of locally generated tsunamis for portions of the Big Island.

5.2 Additional instruments should be installed near the margins of HAVO's boundaries for more comprehensive and necessary coverage.

5.3 The "campground siren system" installed at Halape needs to be modified with satellite remote control capabilities and a louder siren for all campgrounds.

5.4 In conjunction with a satellite remote controlled siren system, the recently installed detection instruments can also provide the basis for warnings of locally generated and Pacific-wide tsunamis at those campgrounds.

5.5 The long term effects of the environment on these installations needs to be evaluated. As such, in the near term, the absence of detected inundation after the occurrence of a nearby earthquake should not be used to infer that a significant tsunami has not occurred.

5.6 However, the detection of inundation after a nearby earthquake should trigger an immediate warning for the Big Island that could be discontinued or expanded as data is received from other instruments.

5.7 Visitors to the campgrounds should receive comprehensive, accurate, and up-to-date information on tsunami hazards.

5.8 Consideration should be given to expanding existing shelters, adding more small individual shelters, or landscaping “tsunami safe sleeping areas” inland and at higher elevations outside of the tsunami inundation zones sufficiently, in terms of privacy or structure, to encourage nighttime use.

The steps taken thus far by HAVO to address tsunami issues represent reasonable and responsible efforts to protect visitors in shoreline areas from tsunami hazards. Further actions suggested in this report should be considered to complete this task.

Acknowledgements

The construction and installation of the instruments was supported by funding given to the State of Hawaii’s Civil Defense Agency by the National Tsunami Hazards Mitigation Program. The work involved was a cooperative effort involving State Civil Defense, the Pacific Tsunami Warning Center, the Hawaii County Civil Defense Agency, Hawaii Volcanoes National Park, and the Hawaiian Volcano Observatory.

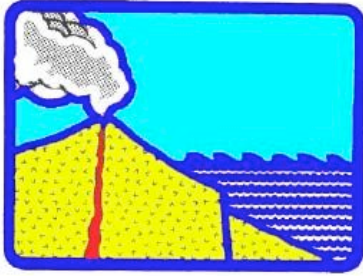
REFERENCES

Cox, D.C., and Morgan, J. (1977). Local Tsunamis and Possible Local Tsunamis in Hawaii, HIG-77-14, Hawaii Inst. of Geophysics, 118 pp.

Lander, J.F., and Lockridge, P.A. (1989). United States Tsunamis (including United States possessions) 1690-1988, National Geophysical Data Center, Publication 41-2, Boulder, Colorado, 265 pp.

Klein, F.W., Frankel, A.D., Mueller, C.S., Wesson, R.L., and Okubo, P.G. (2001). Seismic Hazard in Hawaii: High Rate of Large Earthquakes and Probabilistic Ground Motion Maps, Bull. Seismol. Soc. Amer., 91, 479 - 498.

Walker, D.A., and Cessaro, R.K. (2002). Locally Generated Tsunamis in Hawaii: A Low Cost, Real Time Warning System with World Wide Applications, Sci. Tsunami Haz. 20, 4, 177 - 182.



**DESIGN LOAD EVALUATION FOR TSUNAMI SHELTERS BASED ON DAMAGE
OBSERVATIONS AFTER INDIAN OCEAN TSUNAMI DISASTER DUE TO THE 2004
SUMATRA EARTHQUAKE**

Y. Nakano

*Professor, Dept. of Fundamental Engineering, Institute of Industrial Science, The University of Tokyo,
Tokyo, Japan Email: iisnak@iis.u-tokyo.ac.jp*

ABSTRACT

Tsunami shelters are of great importance to mitigate casualties by earthquake-induced killer waves, and the design guidelines for their practical design are recently developed by a task committee under the Japanese Cabinet Office, since great earthquakes significantly affecting coastal regions are expected to occur in the near future in Japan. Although they propose a practical design formula to calculate tsunami loads acting on shelters, it is derived primarily based on laboratory tests with scaled models but not on damage observations. It is therefore essential to examine the design loads through comparison between observed damage and structural strength. In December 2004, a huge scale Sumatra Earthquake caused extensive and catastrophic damage to 12 countries in the Indian Ocean. The author visited Sri Lanka and Thailand to survey structural damage due to tsunami, and investigated the relationship between damage to structures, lateral strengths computed based on their member properties, and observed tsunami heights. In the survey, 28 simple structures generally found in the affected coastal regions were investigated. The investigated results show that the design tsunami loads proposed in the guidelines are found rational to avoid serious damage but may not be conservative if the load amplification due to drifting debris is taken into account.

KEYWORDS: 2004 Sumatra Earthquake, tsunami shelter, design load, damage survey, inundation depth

1. INTRODUCTION

Mitigating damage due to tsunami as well as due to strong ground shaking is of highest priority to minimize loss of human lives and properties in areas along the coastline susceptible to tsunami hazard. Since great earthquakes such as Tokai Earthquake and Tonankai-Nankai Earthquake significantly affecting coastal regions are expected to occur in the near future in Japan, a task committee was set up under the Japanese Cabinet Office to discuss requirements and criteria to identify or design tsunami shelters and the design guidelines for tsunami shelters were proposed in 2005 (JCO 2005). The guidelines introduced an equation to compute tsunami loads expected to act on shelters constructed on coastlines, which is currently the only formula in Japan available for practically evaluating design tsunami loads for shelters. The equation was, however, developed primarily based on laboratory tests of 2-dimensional scaled model (Asakura et al. 2000) and has not yet been verified through damage observations after natural earthquake-induced tsunamis. It should also be noted that few damage investigations have been made focusing on quantitative evaluation of tsunami loads on building structures unlike that of seismic loads in the building engineering field. The author therefore made extensive damage surveys of structures that experienced the 2004 Indian Ocean Tsunami to investigate the relationship between their lateral resistance and observed damage, and to verify the appropriateness of the design equation. In this paper, the outline of damage surveys and investigated results on design tsunami loads is presented.

2. DAMAGE SURVEYS

2.1. Surveyed Areas

Damage surveys were made in (1) the northeast and south of Sri Lanka (Trincomalee, Galle, Matara, Hambantota etc.) on February 19 through 26, 2005 and (2) Phuket Island and Khao Lak of Thailand on March 9 through 13, 2005. Figure 1 shows the epicenter and surveyed areas. They are located about 1600 km and 500 km away from the epicenter, respectively, and have been little affected by ground shaking (Nakano 2007).

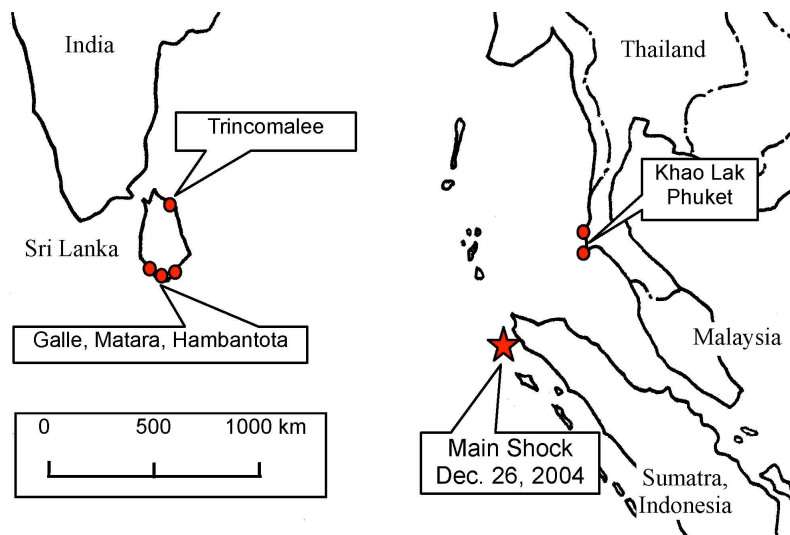


Figure 1 Epicenter and investigated areas

2.2. Survey Strategy

To collect as many damage data as possible for various types of structures and their structural properties, damage surveys were made at approximately 80 sites. Of the all surveyed structures, detailed surveys were made on 28 structures to record structural dimension and reinforcement arrangement to further investigate the relationship between their lateral resistance and tsunami load that acted on them since they met the following three conditions:

- (1) The lateral resistance of the surveyed structures could be simply estimated based on the structural properties obtained on site, because (i) their sectional properties (cross-sectional size, reinforcement arrangement, etc.) were measured; (ii) their damage (or collapse) mechanism was simple and the boundary between damaged and intact part of the structure was not complicated; and (iii) they were small and/or regular enough in their plan and height that their lateral strength could be calculated through simple modeling and assumptions.
- (2) The tsunami trace height was clearly found on the surveyed site through water marks left on building's walls, where it was defined as the water depth above the ground level (i.e., inundation depth) at the structure's site. In addition to that, on-site interviews were also made to enrich tsunami inundation depth data if available.
- (3) The tsunami load could be simply estimated because the surveyed structures were located in areas close to the coastlines and the direct effects by tsunami attack were the primary source of the damage.

Note that drifting debris as well as tsunami waves may have caused damaging impact on structures. Their effects were therefore considered in investigating the relationship between damage category and lateral resistance when the collision of debris was found to have obviously affected the damage to the surveyed structure.

2.3. Detailed Information Recorded on Surveyed Structures

Considering conditions for detailed surveys described earlier in 2.2, (a) building structures with simple configuration, (b) masonry (brick or concrete block) fence walls, (c) cantilever RC columns, (d) elevated water tanks supported by four columns, (e) Buddha's small mausoleums, and (f) small brick structures such as outhouses (i.e., outdoor toilets) and sheds were investigated for collecting detailed structural information. In the detailed surveys, the following data were collected at each site: (1) topographical information of the site, (2) maximum tsunami inundation depth obtained through measurement and, if necessary, supplementary on-site interviews, (3) building's use and structural type (RC, brick, concrete block, etc.), (4) damage category (no damage, cracked, or collapsed) and damage location(s), (5) structure and/or member dimension (B x D x H etc.), (6) reinforcement arrangement (diameter, spacing, cover concrete depth etc.), if it was an RC structure, and (7) general view photos and structural configurations of investigated structures.

Table 1 summarizes the investigated structures and photo 1 shows their typical damage patterns. Note that the structures categorized in (d) through (f) described above were generally found in the affected areas in Sri Lanka, and their data were collected to identify the criteria between damaged and survived structures even if they had minor or no damage. Detailed damage descriptions of surveyed structures and their structural information can be found in the related report (Nakano 2005).

3. EVALUATION OF LATERAL RESISTANCE OF INVESTIGATED STRUCTURES

According to the damage and failure mode observed, the flexural yielding strength M_y , the ultimate flexural strength at rebar fracture M_u , the overturning strength MT , and the shear strength V_u are calculated, where M_y and M_u of RC members are computed from Eqs. (3.1) through (3.3) that are usually applied to beams and columns in Japanese design practice shown as follows:

$$M_y = 0.9 \sigma_y d \quad (3.1)$$

$$M_u = 0.9 \sigma_u d \quad (3.2)$$

$$M_y = 0.8 \sigma_y D + 0.5 N D [1 - N / (B D F_c)] \quad (3.3)$$

where M_y and M_u are the flexural yield strength and the ultimate flexural strength, respectively; σ_y and σ_u are the yield strength and the tensile strength of rebar, respectively; a is the cross-sectional area of tensile rebars; B , D , and d are the width, the depth, and the effective depth of a section, respectively; F_c is the compressive strength of concrete; and N is the axial load.

Note that most of columns investigated herein have low axial loads and their flexural resistance is evaluated from Eqs. (3.1) and (3.2) neglecting the axial load contribution to resistance while Eq. (3.3) is applied in calculating lateral resistance of a 2-story building designated by S53 in Table 1 (see also (8) in photo 1). It should also be noted that the factor 0.8 in Eq. (3.3) is modified according to the ratio of cover concrete to depth observed in the structure since the cover is thicker than the construction practice generally found in Japan. In computing the strength, the yield and tensile strength of reinforcing bars (σ_y and σ_u in Eqs. (3.1) through (3.3)) are determined from tensile tests of sample rebars (two samples from buildings in Sri Lanka and six samples from those in Thailand) that are carried out in Japan. The shear strength V_u of brick walls is defined as the product of its cross sectional area A_w in the principal direction of the structure along tsunami attack and the ultimate shear stress τ_u , where τ_u is assumed 0.4 N/mm² considering the wall's configuration and the brick's quality generally found in the affected areas. The contribution of walls in the direction perpendicular to the tsunami attack is neglected. In calculating the lateral resistance of 2-story building S53, the load-deformation relationship is assumed to reach its peak when the brick fails. The contribution of RC columns to the overall resistance is therefore reduced to half of their ultimate strength assuming the compatibility of deformation between stiffer brick and softer RC columns, which is consistent with the assumptions found in the Japanese Standard for Seismic Evaluation of Existing RC Buildings (JBDPA 2005).

Table 1 Strength, coefficient α , and damage of investigated structures (shaded rows denote column-shaped structures)

ID	Description of structures	Structure type ¹	Location	M_f, M_s, M_r (kNm)	F_h (kN)	Inundation depth H_{max} (m) ²	Coeff. α ³	Damage ⁴	Remarks
S01	Column at entrance gate	RC	Trincomalee	$M_f: 20$	—	(3.0)	1.98	○ (×)	Possibly damaged by drifting debris
S06	Fence wall (1)	RC+B	Trincomalee	$M_f: 40.5$	—	0.9	1.70	×	Just on coastline
S08	Wall of out-house (1)	B	Trincomalee	$M_f: 35$	—	1.3	2.38	×	Bond failure of mortar between brick units considered in M_f
S12	Fence columns	RC	Galle, cricket field	$M_f: 6.6$	—	3.0	1.13	×	Possibly damaged by drifting debris
S15	Columns supporting elevated water tank (2)	RC	Galle	$M_f: 104$	—	2.4	3.03	(×)	Damaged by a drifting bus
S16	Cast/lever columns of automobile factory's office	RC	Galle	$M_f: 26$	—	2.4	1.76	○	No damage unless hit by a bus
S19	Fence wall (2)	RC+CB	Galle	$M_{sc}: 33$	—	2.4	2.04	○ (×)	CB wall neglected in M_{sc}
S23	Wall of nursery school	B	Galle	$M_{sc}: 135$	349	2.35	1.01	×	CB wall neglected in M_{sc}
S24	Wall of small shed (1)	B	Galle	—	480	1.55	4.03	(△)	Scratch found on wall, possibly damaged by drifting debris
S25	Wall of out-house (4)	B	Galle	—	130	1.6	>5.0	○	Located just behind S23
S26	Mausoleum of Buddha (3)	B	Galle	—	182	1.6	3.68	○	Located just behind S23 / Entry perpendicular to tsunami direction
S26	Mausoleum of Buddha (3)	B	Galle	—	182	1.6	>5.0	○	Located just behind S23
S32	Columns supporting elevated water tank (3)	B	Hambantota	—	9.5	2.95	0.54	×	Bond failure of mortar between brick units considered in F_h
S33	Wall of out-house (5)	B	Hambantota	—	83	0.95	4.07	○	Entry perpendicular to tsunami direction
S37	Columns supporting elevated water tank (4)	B	Hambantota	—	305	2.6	4.42	○	Far from coastline
S38	Columns supporting elevated water tank (5)	B	Hambantota	—	925	(5.0)	2.92	○	
S45	Wall of out-house (7)	B	Kotigoda	—	170	(3.0)	2.35	○	Entry perpendicular to tsunami direction
S46	Wall of small shed (2)	B	Motara	—	263	2.05	3.98	○	Entry perpendicular to tsunami direction
S48	Wall of out-house (9)	B	Motara	—	90	2.05	2.22	○	Entry perpendicular to tsunami direction
S53	School building	RC+B	Motara	—	1316	2.85	2.31	○	Entry perpendicular to tsunami direction
S57	Cast/lever columns (1) under construction	RC	Hikkadiva	$M_f: 18$	—	(9.0)	0.54	×	2-story RC building / Seismic capacity evaluation performed
T01	Wine cellar's wall	B	Pinang Beach	$M_{sc}: 23$	—	(9.0)	0.99	×	Of all 15 columns, 8 totally collapsed and 7 heavily damaged
T02	Kanala Beach H&R	RC+B	Kanala Beach	—	680	1.75	>5.0	○	Approx. 100m away from coastline
T07	Fence columns (1)	RC	Thap Lamu, Phang Nga	$M_f: 30$	1473	3.95	(1.60)	○	Approx. 60m away from coastline (not plotted in Figure 4)
T09	Fence columns (2)	RC	Thap Lamu, Navy Base	$M_f: 4.5$	—	2.65	0.43	×	Pull-out of round rebars observed / Approx. 1km from coastline
T10	Columns of pier house (next to Navy Base)	RC	Thap Lamu, Phang Nga	$M_{sc}: 6.3$	—	2.65	1.39	×	Pull-out, yielding, and fracture of round rebars observed / Approx. 1km from coastline
T13	Guest house of Khao Lak Merin Resort Hotel	RC+B	Phang Nga	$M_f: 4.7$	—	2.65	0.98	×	Yielding and fracture of round rebars observed / Just on coastline
T15	RC columns of La Fira Khao Lak Hotel	RC	Phang Nga	$M_{sc}: 6.6$	317	4.23	1.36	△ ×	Brick wall ($F=380\text{cm}$) considered in F_h
T17	Cast/lever columns (3) under construction	RC	Phang Nga	$M_f: 12.9$	—	5.0	0.70	×	Of 11 guest houses, 9 collapsed or washed away
				$M_{sc}: 19.9$	—	5.0	0.87	×	Just on coastline
				$M_{sc}: 28.6$	—	3.3	1.62	×	Far from coastline (estimated at more than 1 km away)
				$M_{sc}: 43.9$	—	3.3	2.02	×	

¹ RC: RC columns; B: Unreinforced (UR) brick wall; CB: UR concrete block wall ² Tsunami inundation depth above ground level (value in () denote estimated depth off or interviews)

³ $\alpha = \text{computed water depth } d_f \text{ at } M_f, M_s, M_r, \text{ or } F_h / [H_{max}]$ ⁴ T02 is not plotted in Figure 4 due to uncertain information of reinforcing details.

⁴ ○: no damage; △: cracked; ×: collapsed or extensively tilted; (): damage due to drifting debris (more than a single mark at an identical plot in Figure 4 denotes occurrence of different types of failure)

4. COMPARISON BETWEEN TSUNAMI LOAD AND OBSERVED DAMAGE

In the guidelines, the design tsunami load is defined by Eq. (4.1). In the subsequent investigations, Eq. (4.2) that is analogous to Eq. (4.1) is first defined, and the coefficient a is evaluated setting the lateral resistance of investigated structure equal to the tsunami load computed from Eq. (4.2):

$$q_x(z) = \rho g (3 h - z) \quad (4.1)$$

$$p_x(z) = \rho g (a \eta_{\max} - z) \quad (4.2)$$

where $q_x(z)$ (kN/m²) is the design tsunami pressure acting on a structure at a distance z above the ground level .



(1) S01: RC columns (2) S08: Brick outhouse (3) S16: Cantilever RC columns with rebar fracture



(4) S19: CB fence wall w/ RC column (5) S25: Brick outhouse (6) S26: Mausoleum (7) S32: Elevated water tank



(8) S53: 2-story RC school (9) S57: RC columns under construction (rebars bent and some columns failed)



(10) T09: RC fence columns of Navy Base (rebar fractured) (11) T15: RC columns under construction

Photo 1 Typical damage to investigated structures ("S01" etc: ID Nos. in Table 1, "→": tsunami flow direction)

defined in the guidelines (JCO 2005), ρ (t/m³) is the mass per unit volume of water (1.0 assumed herein), g (m/s²) is the gravity acceleration, h (m) is the design tsunami inundation depth, z (m) is the distance above the ground level to compute tsunami pressure p_x and q_x ($0 < z < 3h$ for Eq. (4.1) and $0 < z < a \eta_{\max}$ for Eq. (4.2)), $p_x(z)$ (kN/m²) is the tsunami pressure acting on a structure at a distance z above the ground level where η_{\max} (m) is the observed tsunami inundation depth, a is the ratio of the water depth η ' equivalent to structure's ultimate strength to the observed tsunami inundation depth η_{\max} (i.e., $a = \eta / \eta_{\max}$). Note that the inundation depth for h and η_{\max} is defined as the water depth above the ground level at the building's location.

Figure 2 illustrates the background concept employed in Eq. (4.1). The design tsunami pressure distribution acting along the structure's height is assumed a triangular shape with the height reaching 3 times of the design tsunami inundation depth h (i.e., the pressure at the bottom is assumed 3 times of the hydrostatic pressure), which is based on the laboratory tests of 2-dimensional scaled model (Asakura et al., 2000). To examine whether or not the coefficient 3 in Eq. (4.1) is appropriate to evaluate the tsunami load, Eq. (4.2) is introduced in the manner analogous to Eq. (4.1). If the coefficient a successfully categorizes damaged and survived structures at its value of 3, one can say that Eq. (4.1) with a equal to 3 is a rational design formula to compute the tsunami load effect. In calculating the coefficient a , two typical cases of inundation depth and structure's height, which can be found in the guidelines (JCO 2005), are taken into consideration as shown in Figure 3 since they are the basic patterns of tsunami attack to existing structures in the surveyed areas.

The coefficient a can be computed assuming that the lateral resistance of an investigated structure is equal to the overall tsunami load acting on it under the pressure distribution along its height defined by Eq. (4.2). The coefficient therefore denotes the ratio of equivalent water depth η ' corresponding to the structure's lateral resistance under a triangular hydrostatic pressure profile to the observed inundation depth η_{\max} . The procedure to compute the coefficient a is described in detail below.

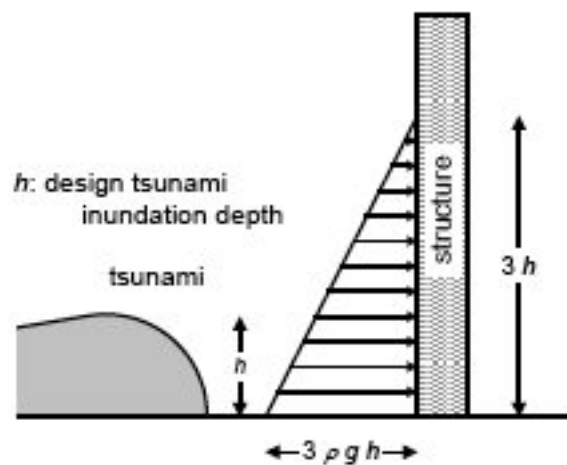


Figure 2 Design pressure tsunami distribution (JCO 2005)

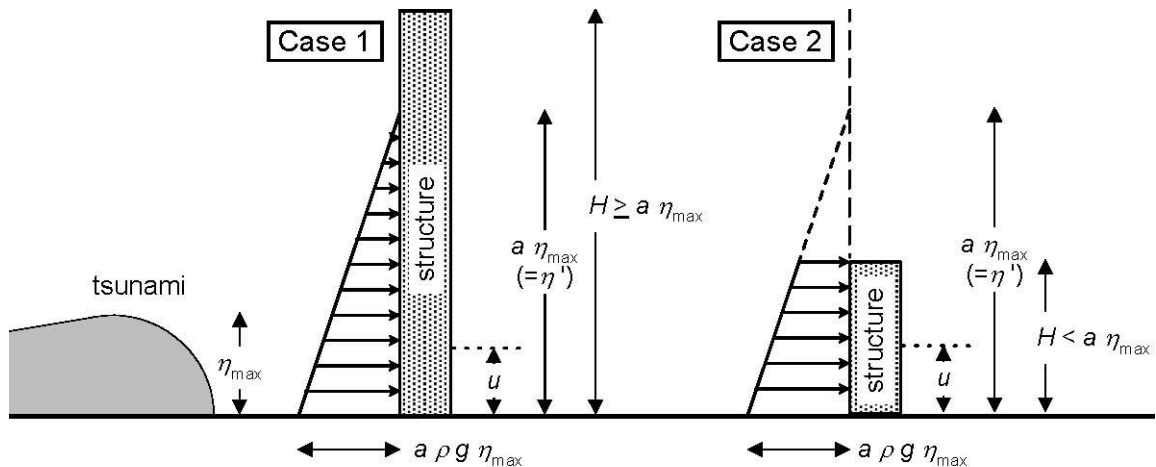


Figure 3 Tsunami inundation depth η_{\max} , building height H , and tsunami pressure distribution p_x (Nakano 2007)

1. Compute the lateral resistance of investigated structures considering their failure mode as shown earlier in Section 3.
2. Then compute shear force or bending moment acting at the failure point u (defined as the distance between the failure point and the ground surface) assuming the tsunami pressure distribution as defined in Eq. (4.2). Setting the force or moment at the height u equal to the lateral resistance obtained in step 1. above, evaluate the equivalent water depth η' corresponding to the resistance. Note that the tsunami pressure above structures is neglected and the depth η' is evaluated assuming the trapezoidal instead of triangular pressure distribution in computing the force or moment as shown in case 2 of Figure 3.
3. Finally compute the coefficient a , which is defined as the ratio of equivalent water depth η' to observed tsunami inundation depth η_{\max} (i.e., $a = \eta' / \eta_{\max}$).

Table 1 shows the investigated tsunami inundation depth η_{\max} and the computed coefficient a . Their relationship is shown in Figure 4(a) for wall-shaped structures such as fence walls and in Figure 4(b) for column-shaped structures such as cantilever RC columns, respectively, where the structure type is determined based on the shape of member on which the tsunami attacks. When the structures with identical structural properties have different failure patterns due to the effects of drifting debris or some other reasons, two marks corresponding to different failure patterns are plotted at the same point of the figure.

Figure 4(a) shows that structures with the value of a greater than 2.5 have no major damage except for the case S23 that may have been damaged due to drifting debris, and the value of 3 for the coefficient a proposed in the guidelines can be considered rational to avoid serious damage due to tsunami attack. It should be noted, however, that the structure (S23) having the coefficient a greater than 4 suffers wall cracking, and the coefficient of 3 may not be conservative if the load amplification due to drifting debris is taken into account, and countermeasures to protect structures from damage due to drifting debris need to be taken.

Figure 4(b) shows that the coefficient a for column-shaped structures to discriminate between damaged and survived may lie at around 2 when the effects of drifting debris are neglected, which is slightly lower than that for wall-shaped structures. This result implies that column-shaped structures have advantage in tsunami resisting performance over wall-shaped structures on condition that both structures have enough seismic capacity to survive the ground shaking prior to the tsunami attack. It should also be noted, however, that the column-shaped structures can not be left undamaged at the coefficient a in the range of 2 to 3 as shown for the cases of S01, S15, and S16, and countermeasures against drifting debris need to be taken to protect structures as is the case of wall-shaped structures previously described

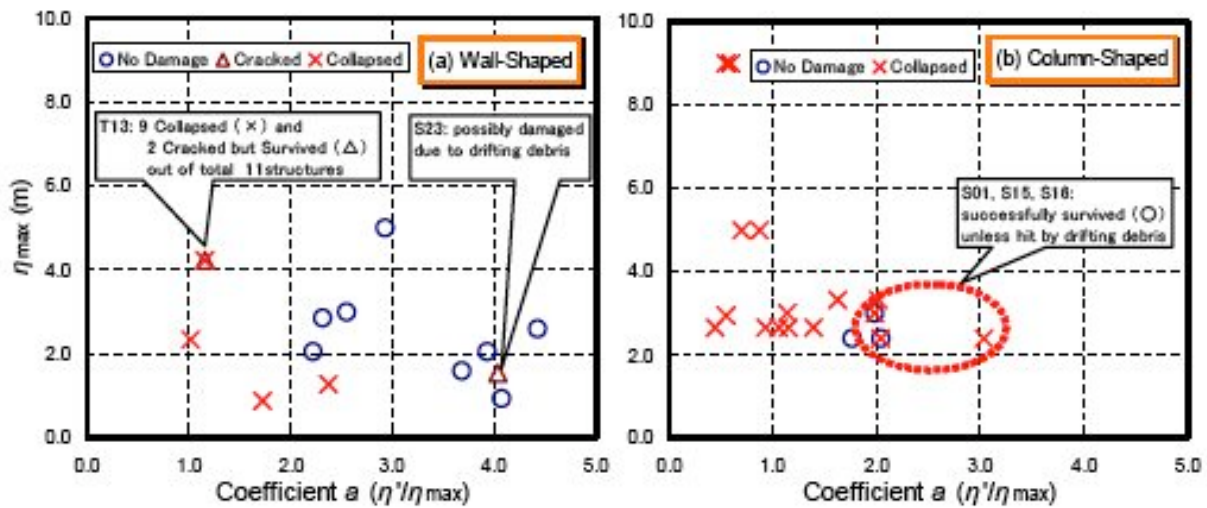


Figure 4 Computed Coefficient a vs. observed tsunami inundation depth η_{max} (Numerals in the figure denote ID Nos. in Table 1)

5. CONCLUSIONS

To examine the design load specified in the Japanese guidelines for tsunami shelters, damage surveys are made in Sri Lanka and Thailand after the 2004 Indian Ocean Tsunami disaster, and the lateral strengths of structures in the affected areas, the tsunami load computed by the design formula considering tsunami inundation depth, and the observed damage are mutually compared. The major findings can be summarized as follows:

1. The value of coefficient 3 for computing design tsunami loads proposed in Eq. (4.1) of the guidelines compares well with the criteria between damaged and survived structures in the tsunami affected areas surveyed after the 2004 Indian Ocean Tsunami disaster, and the design tsunami load specified in the guidelines is found rational.
2. The value, however, may not be conservative if the load amplification due to drifting debris is taken into account, and other countermeasures would be needed to avoid unexpected damage due to debris.

ACKNOWLEDGEMENTS

This research was partially funded by 2004 Grant-in-Aid for Promotion of Science and Technology (Project title: Urgent Research on Damage due to Sumatra Earthquake and Indian Ocean Tsunami; Sub-theme: Vulnerability Investigations Related to Earthquake-Induced Tsunami Disasters led by Dr. K. Meguro, Prof. of Institute of Industrial Science, The University of Tokyo) and TOSTEM Foundation for Construction Materials Industry Promotion (Project title: Design Tsunami Load Evaluation and Data Archives Based on Field Surveys after Devastating Tsunami Disaster due to 2004 Sumatra Earthquake, Grant No. 05-26 (2005), Y. Nakano, Principal Investigator). The field surveys were made under extensive cooperation with Dr. G. Shoji, Assistant Professor of Tsukuba University; Mr. Ganila N. Paravithana, Central Engineering Consultancy Bureau, Sewerage Engineering, Sri Lanka; and Mr. Perapol Begkhuntod, Thai Meteorological Department, Thailand. The author gratefully acknowledges their valuable supports to complete the research project.

REFERENCES

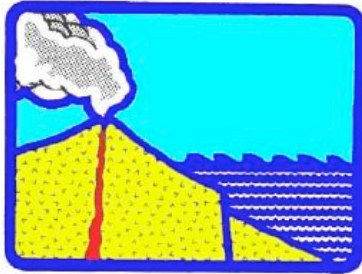
Asakura, R., Iwase, K., Ikeya, T., Takao, M., Kaneto, T., Fujii, N., Omori, M. (2000). An Experimental Study on Wave Force Acting on On-Shore Structures due to Overflowing Tsunamis, Proceedings of Coastal Engineering, Japan Society of Civil Engineers, 47, 911-915.

JBDPA/Japan Building Disaster Prevention Association (2005). Standard for Seismic Evaluation of Existing Reinforced Concrete Buildings, 2001; Guidelines for Seismic Retrofit of Existing Reinforced Concrete of Existing Reinforced Concrete Buildings, 2001; Technical Manual for Seismic Evaluation and Seismic Retrofit of Existing Reinforced Concrete Buildings, 2001, English Version, 1st.

JCO/Task Committee under the Japanese Cabinet Office (2005). Design Guidelines for Tsunami Shelters (in Japanese), http://www.bousai.go.jp/oshirase/h17/tsunami_siryu2.pdf Nakano, Y. (2005). Damage Report on Structures due to 2004.12.26 Sumatra Earthquake Ver. 2.2, <http://sismo.iis.u-tokyo.ac.jp/Research.files/topic4.files/topic4-007.files/T4-7-1.pdf>

Nakano, Y. (2007). DESIGN LOAD EVALUATION FOR TSUNAMI SHELTERS BASED ON DAMAGE OBSERVATIONS AFTER INDIAN OCEAN TSUNAMI DISASTER DUE TO THE 2004 SUMATRA EARTHQUAKE, Journal of Architecture and Building Science, Architectural Institute of Japan, 13: 25, 337-340.

ISSN 8755-6839



SCIENCE OF TSUNAMI HAZARDS

International Journal of the Tsunami Society

Volume 29

Number 1

2010

A STUDY OF THE EDGE WAVE EFFECTS INDUCED BY THE TSUNAMI OF 26 DECEMBER 2004 AT PHI-PHI ISLAND IN THAILAND

R.H.C. Wong, H.Y. Lin, K.T. Chau and O.W.H. Wai

Department of Civil & Structural Engineering, The Hong Kong Polytechnic University, Hong Kong, CHINA
Email: cerwong@polyu.edu.hk

ABSTRACT

The present study compares experimental laboratory results of the edge wave effect along Phi-Phi Island in Thailand with field-trip observations taken after the 26 December 2004 tsunami. A physical model of the island was constructed, with vertical scale of 1:500 and horizontal scale of 1:2500 in a 6×6 m steel tank. Waves were generated by the sudden opening of a gate releasing water from an elongated rectangular reservoir (6m×0.5m×0.6m). The initial tank water level was adjusted to simulate tsunami waves of various heights. The experimental observations focused on input wave heights, speed of propagation and the effect of edge waves on tsunami run up heights. The results explain how edge wave propagation was strongly affected by the size and shape of Phi-Phi Island and how it contributed to greater destruction. Additionally, the experimental observations provide valuable benchmark results that can help calibrate and validate numerical tsunami models.

KEYWORDS: Edge wave, Phi-Phi Island, tsunami, run up height, tombolo,

Science of Tsunami Hazards, Vol. 29, No. 1, page 21 (2010)

INTRODUCTION

The tsunami generated by the December 26, 2004 earthquake ($M_w=9.3$) near the coast of Sumatra (Fig.1a) killed over two hundred twenty thousand people. The earthquake resulted from crustal movements along a region where the Indian/Australian tectonic plate subducts the Burma subplate of Eurasia (Fig. 1b). Research was undertaken because of concern that Hong Kong and other coastal regions of the South China Sea may be also vulnerable to future tsunami impact from earthquakes where the Eurasian and Philippine tectonic plates collide – a region known for frequent seismic and volcanic activity. As part of this research in evaluating potential tsunami risks, a 4-day field survey was made to Phuket and Phi-Phi Island in Thailand, from Feb 4-7, 2005, for the purpose of examining tsunami damage along the coastline of the island (Fig.2). The present study focuses on experimental modeling of tsunami effects at Phi-Phi Island and compares the results with what was observed in the field, for the purpose of obtaining a better understanding of how edge waves associated with a tsunami, could potentially affect and impact Hong Kong. The present paper is divided into three sections. The first describes briefly field observations of edge wave induced by the tsunami at Phi-Phi Island. The next summarizes previous studies of physical hydraulic modeling of edge waves. Lastly, the third section provides details of the physical modeling on how edge wave affected the coastline of Phi-Phi Island.

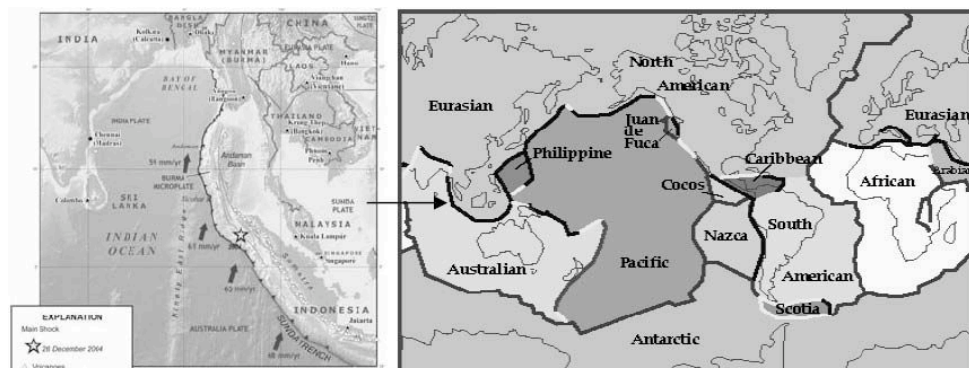


Figure 1 (a) Source Region of the 2004 earthquake; (b) Major tectonic plates.

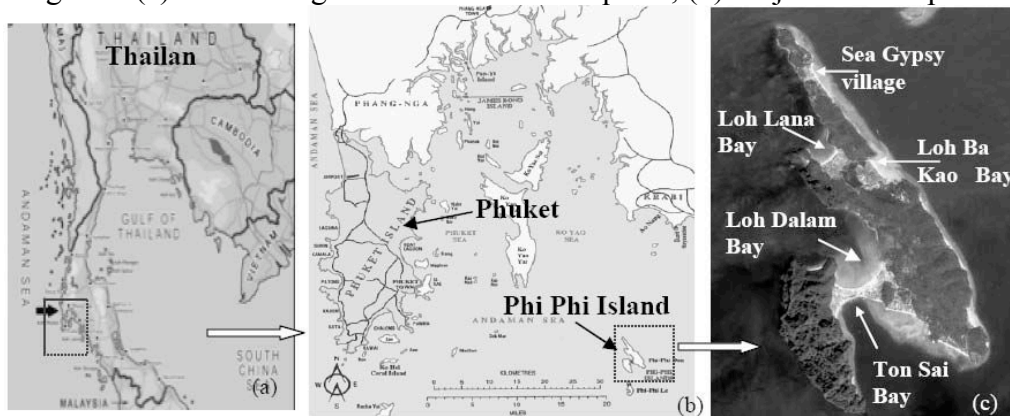


Fig. 2 Location of Phuket and Phi Phi Island in Thailand.

2. FIELD RECONNAISSANCE - PHI PHI ISLAND

Phi-Phi Island consists of two small narrow islands connected with a tombolo as shown in Figure 2c. The orientation of the two islands is roughly in a NNW direction. The length of the easternmost section of the island is about 8 km with the width ranging from 1 to 2 km. The geological formation consists of mudstone and sandstone. The length of the westernmost section of the island is about 3 km with the maximum width of about 1 km. The primary rock formation is limestone. As indicated by the color of water in Fig. 2c, the water depth on the southern side of the tombolo (Ton Sai Bay) is deeper than the northern side (Loh Dalam Bay). The field investigation documented very localized tsunami-induced damages along the coastline of the island. Figure 3a shows the degree of erosion induced by the tsunami along the coastline of the northern part of Loh Lana Bay and the huge boulders that were transported on land. A huge boulder with dimensions of 3m×3m×2m (Fig. 3b) was uplifted to the location marked as 'A' (Fig. 3a) which is also an outlet which allowed water surges to flow over land to the eastern side (the Sea Gypsy Village). An intact plastic bottle and some intact small pebbles supporting the huge boulder, suggest that it was not deposited there by rock all from the slopes above, but that it was transported to this location by tsunami wave action (since there is no evidence of crushing on the contact points). Judging from the size of the boulder, the tsunami's water flow velocity must have been extremely high in this area (approximately 20m/s). Furthermore, the directional bending of the piers, confirmed that the tsunami flow was from west to east (Fig. 3c).

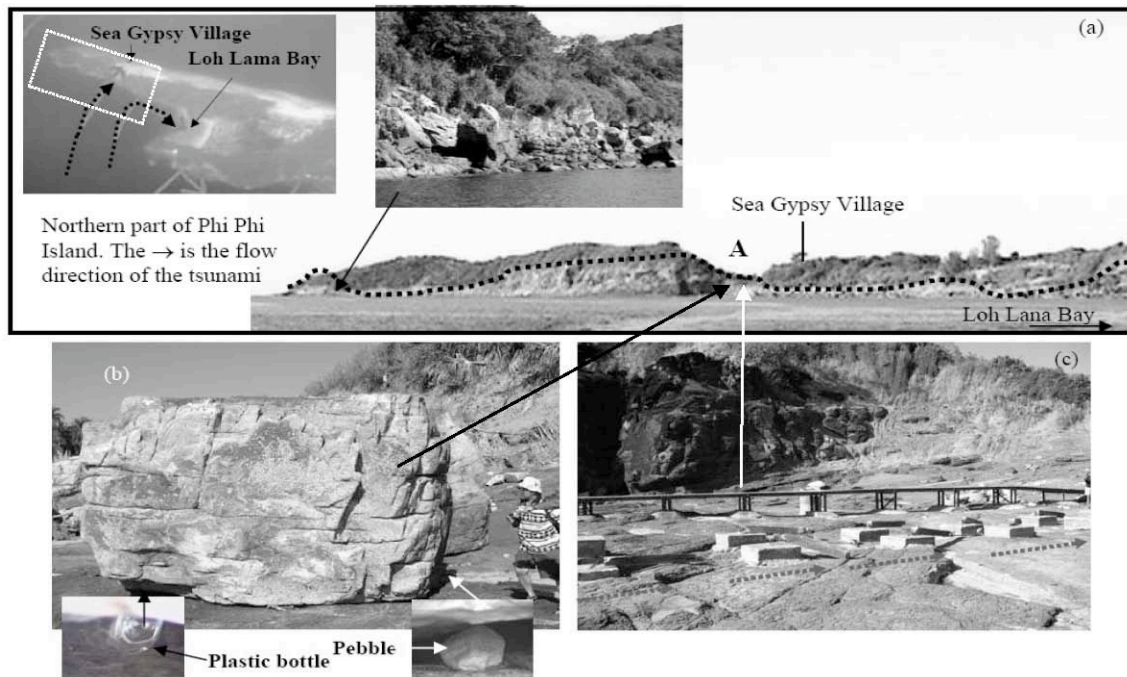


Fig. 3 (a) Non-uniform tsunami run-up height along the northern coastline of Loh Lana Bay. (b) Small photos showing transport of boulders by the tsunami with an undamaged plastic bottle and pebbles underneath the huge boulder. (c) Bent piers indicating tsunami flow direction.

Both north and south sides of the tombolo suffered extensive damage. Internet photos (Fig. 4) indicate that the tsunami came from the north side of the tombolo (Loh Dalam Bay, Figs. 4a & 5a). The run-up height reached the second floor of the hotel there (Fig. 4b) and overflowed the tombolo towards Ton Sai Bay (Figs. 4c & 5a). It is believed that the higher run-up was the result of Loh Dalam bay's deeper bathymetry and coastal configuration. Figure 4c shows the tsunami wave retreating northward to the sea. The enlarged small photo at Fig. 4c shows debris floating in Ton Sai Bay. Eyewitnesses stated that tsunami waves approached the tombolo from both north and south directions. By measuring the scar on top of coconut trees there, the maximum tsunami run-up height was determined to range from 14 to 16 meters (Fig. 5b). Coral boulders with diameters ranging from 1-3 m were uplifted by the tsunami on the north side of the tombolo (Fig. 5c). Figure 5d shows a toppled 2-meter high statue on a pedestal. The steel bars connecting the statue and the stand were all bent in a SE direction, indicating that the stronger tsunami waves came from the north side of the tombolo.

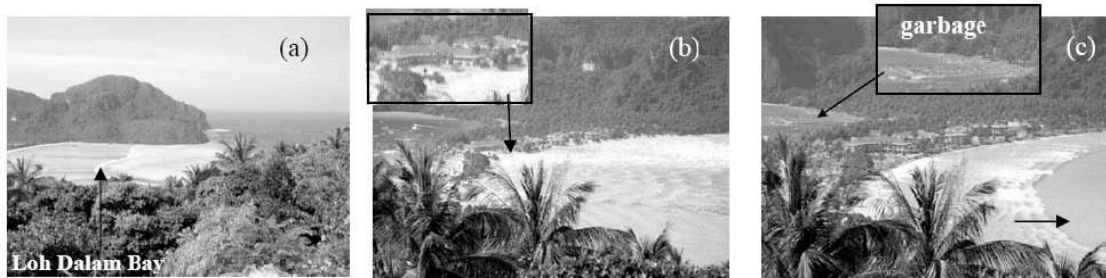


Fig. 4 (a) Tsunami approaching from the north side of tombolo (b) tsunami impacting the north side of tombolo and causing overflow, (c) wave retreating northward with lots of debris floating on the south side of the tombolo

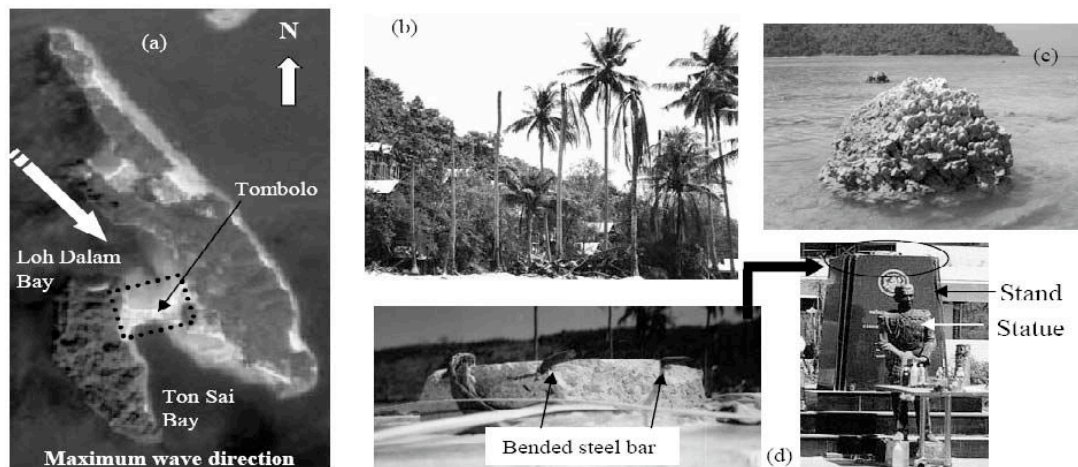


Fig. 5. Tsunami damage on north and south side of tombolo.

These observations raise the question as to why the island to the left of the tombolo was sheltered from tsunami surges. Why did the tsunami wave propagated around the island and impacted to a greater extent the tombolo from both north and south directions?

In fact, similar localized run-up of tsunami has been observed during other great tsunami events elsewhere. Hilo on the Island of Hawaii is the worse affected location every time a tsunami strikes. Weigel (1970) used the results of a physical hydraulic model (scaled 1:5,000) to demonstrate that edge waves (trapped waves traveling along the coastline caused by the superposition of the reflected tsunami with the incoming surges) is responsible for tsunami directional focusing effect there and for the highly localized tsunami run-up heights. The tsunami recorded at Hilo on February 8, 1963 traveled from the east and had a period of 16 minutes. The lines of “Mach stem” or “lines of trapped edge waves” were observed by filming the experiments. The wave run up heights depended on bathymetry and slope of the offshore region, on coastal morphology and on resonance (Wiegel, 1970). The generation mechanism of trapped edge waves was studied extensively to determine its effect on localized tsunami run-up along an irregular coastline (Wiegel, 1970; Dudley and Lee 1998, Bryant, 2001). The edge wave pattern can be duplicated in the laboratory by using a hydraulic model of 1:5,000 scale. Dudley and Lee (1998) reported that a physical model of Hilo harbor with horizontal scale of 1:600 and vertical scale of 1:200 had been used to model the tsunami. Our preliminary observations at Phi-Phi Island suggested that the edge wave phenomenon might be used to explain some of the field observations. Evidently, there were many complex wave reflections that interacted with the incoming trains of the tsunami, in a way that an edge wave was formed. The flow velocity of such edge wave was particularly high and may reflect what actually happened on Phi-Phi Island. Thus, the purpose of our study was to perform laboratory tests to simulate the propagation of the edge wave along the coastline of Phi-Phi Island and compare the results with data from field observations. The scale of the physical model that was used for this investigation was constrained by laboratory space limitations at the Hong Kong Polytechnic University. The model was designed in a way that the size of tsunami and its incoming direction could be adjusted as much as possible. The intent was to use parametric studies to examine the complex interactions created by the local bathymetry, the size and shape of the island and the tsunami wavelength. At the conclusion of the experiments it was determined that the modeling results not only provided good understanding of the effects of edge waves at Phi-Phi Island during the 2004 tsunami, but also provided some insight on the potential tsunami hazard for Hong Kong, where the irregular coastline is would be conducive to the formation of edge waves, if a tsunami strikes.

3. PHYSICAL MODELING AND EXPERIMENTAL SETUP

The physical model of Phi-Phi Island (Fig. 6a) was constructed from corrugated paperboards, each with a paper thickness of 0.6 mm. For a physical hydraulic model, it is normally impossible to have a 1-to-1 vertical and horizontal scale. Some kind of distortion of the vertical scale seems acceptable to avoid the effects of capillary rise and surface tension of the water. Previous experimental studies normally used a scale ratio h/v (horizontal scale/ vertical scale) ≤ 4 , so that the distortion due to the scale effect can be negated (Whalin and Chatham, 1976). However, due to the limited space of the laboratory, an h/v ratio of 5 was used by this study with the horizontal scale being 1:2,500 and the vertical scale being 1:500 for the submerged portion of the model but remains at 1:2,500 scale for the portion above water level. The island was scaled down to about 3m in length and 1.5m in width. The whole model was fixed in a 6m×6m×0.3m (length×width×height) lower steel tank (Fig. 6b).

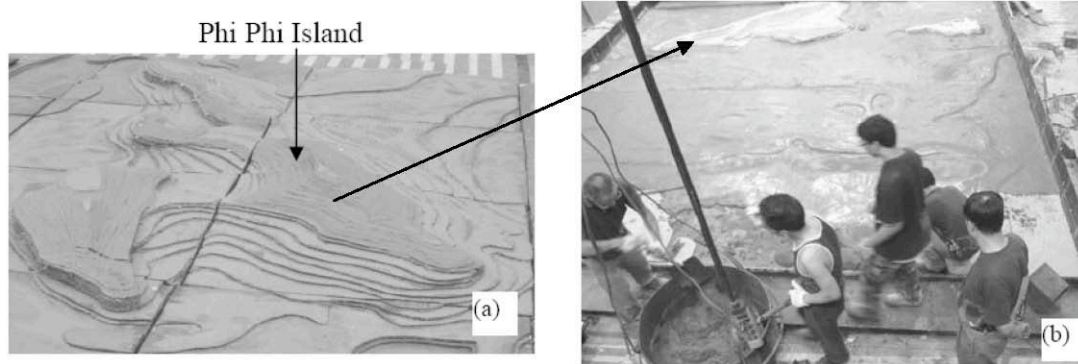


Fig. 6 (a) Model of Phi Phi Island, (b) Submerged portion of the model being covered with a layer of concrete (Model of the island fixed within a 6m×6m×0.3m steel tank).

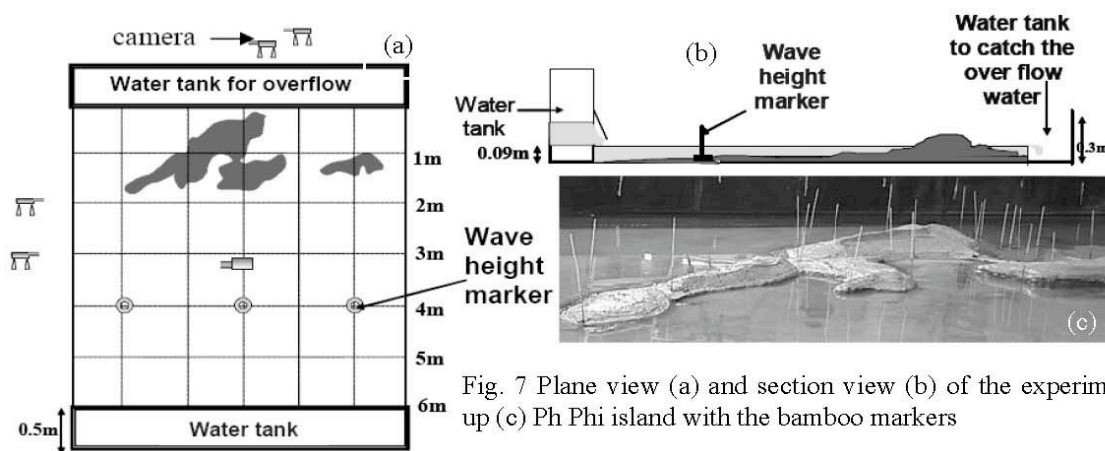


Fig. 7 Plane view (a) and section view (b) of the experimental set up (c) Ph Phi island with the bamboo markers

The physical model, including the island and the submerged portion, were covered by a layer of concrete. After the cement paste is hardened, Water was added to the tank to an approximate level of 90 mm. A separate water storage tank of 6m×0.5m×0.6m (called tsunami tank hereafter) was constructed to serve as the source of tsunami waves and was placed at the far end of the model (Fig.7). A gate was installed at the lower part of the tsunami tank for the sudden release of the water and the generation of simulated waves. The water tank was built on movable rollers outside the model so that the angle of tsunami direction could be adjusted. To prevent wave reflections from the two sides and the opposite wall of the model, a soft 60 mm thick water-absorbent material was mounted on all three sides with an overflow edge at the far end to prevent reflections from behind Phi-Phi Island replica. Wave height markers (Fig. 7a) and bamboo markers (Fig. 7c) were installed to measure the height of the waves and the run-up on the island. Additionally, five video cameras were installed at different locations to record the formation of edge waves and the maximum run-up in the model. Simulated waves were generated having heights varying form 30mm, 40mm and 50mm. Some of the results of our experimental observations are given in the next section.

4. THE EFFECT OF COASTAL MORPHOLOGY ON EDGE WAVE PROPAGATION

Figure 8 shows a sequence of photographs taken from the top of the model, illustrating the wave propagation toward the island. For this particular experiment, the water depth in the tsunami tank was 40 mm with an orientation of $N0.0^\circ$. Once the gate was opened, a line of water was generated and propagated toward the island. Initially observed was the formation of a zone of water level depression (or water draw back) ahead of the first crest, which agreed with observations in Thailand that the sea retreated prior to arrival of the first tsunami wave (see elongation of light reflection before the wave in Fig. 8). The same phenomenon has been observed with many tsunamis in the past – specifically that a wave of higher crest is followed by a number smaller undulations. A mathematical wave called soliton has a similar waveform, similar to a tsunami. Another observation was the reduction of wave speed due to changes in bathymetry. The waves refracted with changes of water depth and coastal configuration. At the tombolo the water first retreated, then rose drastically. At wave marker (2 m away from the water tank), the average wave height was about 14 mm above mean water level, while the wave run up height at the tombolo was 21 mm at the south side and 30mm at the north side. The wavelength was about 0.45 m. The wave speed, at 1 m away from the tsunami tank, was 1.13 m/sec and it decreased to 0.73 m/sec at 2.5m from the tsunami tank. As illustrated by the modeling study and presented in detail in the next section, depth of water and coastal morphology are critical factors in the resulting tsunami run up.

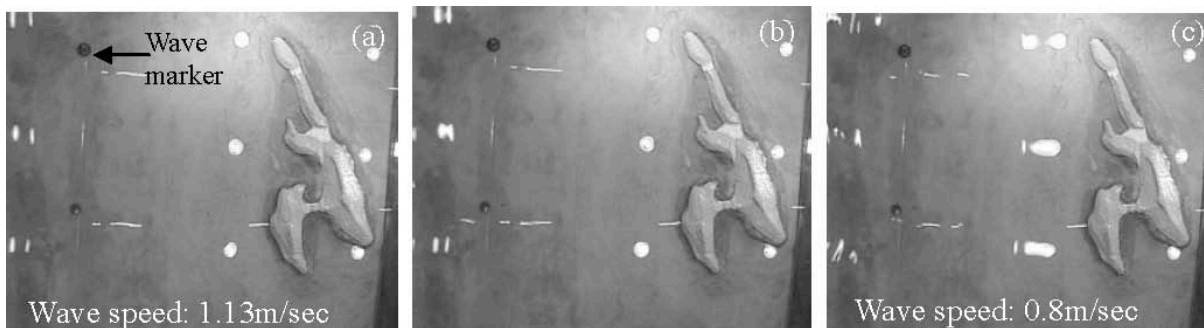


Fig. 8 Wave propagation and interaction with coastal morphology in the generation of edge waves

5.1. Wave attack on the northern coastline of Loh Lana Bay

The topography of the northern side of Phi-Phi Island consists of a flat land 'A' in-between two small hills (Fig. 9a and 9d). When wave propagates toward this area, it was observed that there is water overflow to the other side of the island (Fig. 9a). As a result, this low-lying area became an outlet for the tsunami surge and drew adjacent water through it (Fig. 9b). The water wave speed in this area could not be recorded but the recorded run-up height was 33 mm above still water level and was higher than what was measured at the tombolo (to be further discussed). This observation provides an explanation why the erosion of the coastline on this flatland of Phi-Phi Island is higher than other parts along the northern coastline (Fig. 9d). In addition to the water overflow, part of the wave (edge wave, see Fig. 9b) traveled along the coastline of the island around the northern tip (see the small

photo of Fig. 9b) moving downward along the backside of the island. On the right side of the flat land 'A', a reflected wave (edge wave) was observed traveling along the coastline and moving towards to the southern bay (Fig. 9c). However, since there is no outlet for the water there, the surge reflected back and interacted with the incoming edge waves to form a highly non-uniform and localized run-up height along the northern coastline. This also explains what we actually observed along the northern coastline of Phi-Phi Island. Therefore, the experiments provided useful insight of what happened in this area when the tsunami of December 26, 2004 struck.

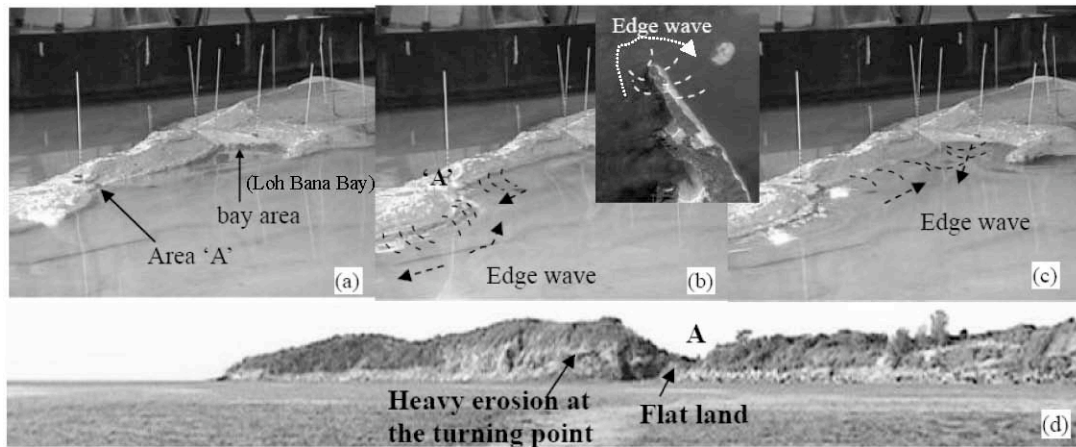


Fig. 9 Illustration showing tsunami wave attack on northern area of the model of Phi-Phi Island

5.2. Wave attack on the Northern Side of the Tombolo (Loh Dalam Bay)

It was observed that when the wave propagated towards Loh Dakam Bay, part of the wave reflected at area B and C (Fig. 10a) while part of the wave moved directly into the bay area. It was observed that at area B, the edge wave moved along the coastline propagating downward to the bay area (Fig. 11b). At the same time the reflected wave (or edge wave) moved along the coastline of area C also propagated toward the bay area (Fig. 11c). As a result, three sources of water flow into the bay area caused the 30 mm run-up height at the north side of the tombolo.

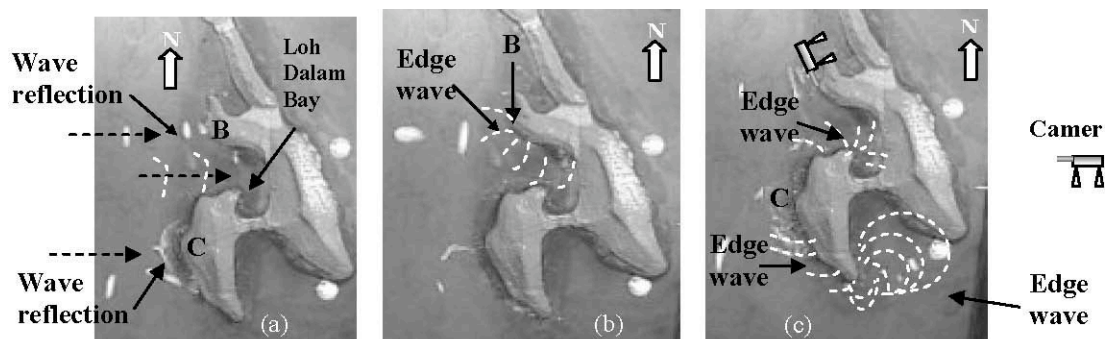


Fig. 10 The plane view of the edge waves moving into the bay area of the north side of tombolo.

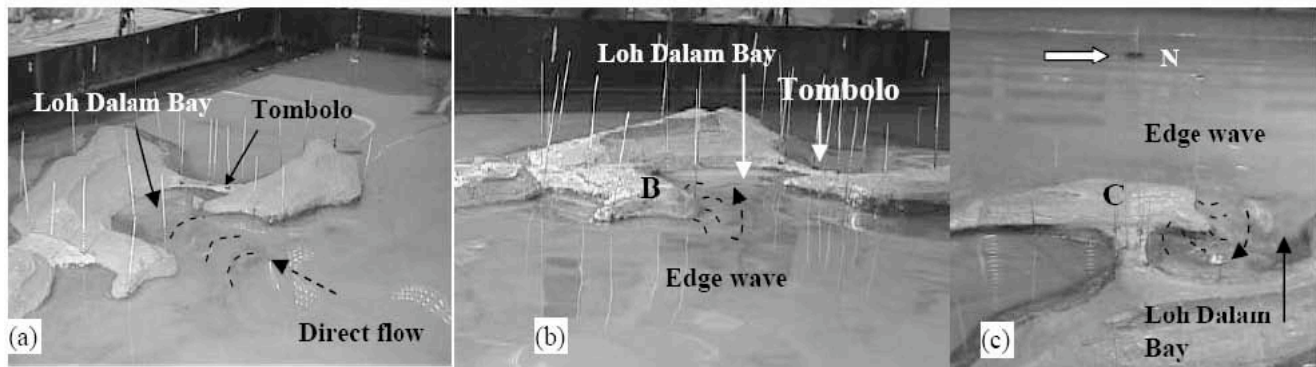


Fig. 11 Photos showing the sources of water from the northern side of the tombolo (Loh Dalam Bay)

To give a clearer picture, three more photos of the Loh Dalam Bay area (Figs. 11a-c) were taken from different angles (locations of cameras shown in Fig. 11c). It was clear that water was coming from three different sources and directions (direct flow, edge wave moving along the coastline of area B and C, respectively). The laboratory observations show that the surge coming from the north of the tombolo was much higher than that from the south, which also agree with field observations that all the damages were caused by surges from the north. The hydraulic model experiments provided a simple reconstruction of what actually happen at Phi-Phi Island and explain why a tombolo which is not directly facing the incoming tsunami, suffered such heavy damage and casualties. It also demonstrates the importance of edge waves on enhancing tsunami run-up.

5.3 Wave attack on the South Side of the tombolo

There is no direct flow source for the south side of the tombolo, since the south bay is sheltered from direct tsunami impact. However, the experiments also show that edge waves were formed and traveled around the left headland. More specifically, when the simulated tsunami wave propagated towards to southern end of the island, it was observed that edge waves were formed that continued to move along the coastline towards to the tombolo (Fig. 11c). Three more photos of the tombolo area taken from different angles are shown in Fig. 13. Figure 13a was taken from the eastern camera while Figs. 13b and 13c were taken form the northern camera. It was observed that edge wave turned around the southern tip of Phi-Phi Island (Fig. 13a) and propagated across to the bay towards the southern side of the other island, with wave fronts nearly parallel to the tombolo (Figs. 13b & c). As a result, the wave arrival time from the south side of tombolo is later than that from the north side. Figure 13c clearly shows that when the surges overflowed the tombolo from the north, the edge wave from the south side was still advancing toward the tombolo. The difference in arrival time on the two sides was about 2.5 sec. Because the source of water from the south was only from the edge wave, the run-up height was only 21 mm. The field observations were in full agreement with the conclusions derived form the hydraulic model experiments. As shown in Figs. 4b and 4c, when the tsunami approached from the north side of the tombolo, the sea on the south side was calm. The debris on the south side resulted by the overflow of water from the north side. That is, wave reached first the north side of the tombolo and the run-up was higher.

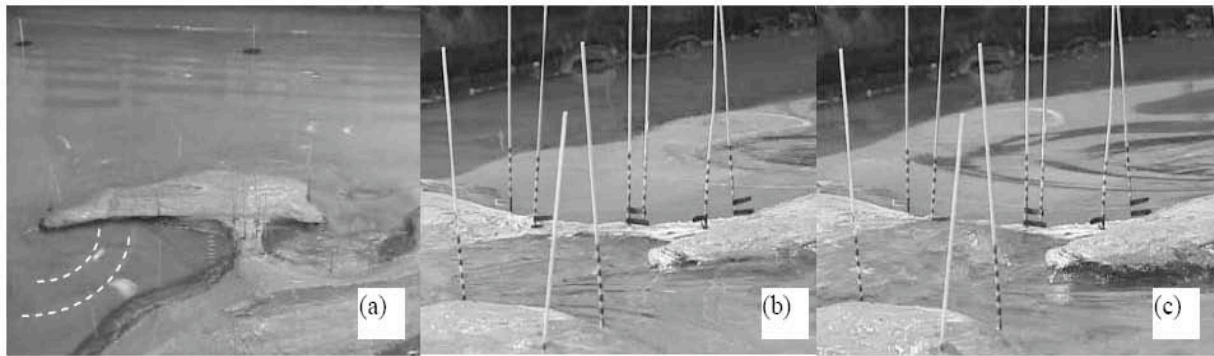


Fig. 12 (a) Edge wave propagation along the coastline, (b) and (c) show the flooding and overflow at the north side of the tombolo while the edge wave propagation from the south side was still going on.

Table 1 summarizes the run-up heights from the model experiments for different initial water depth in the tsunami tank (30mm to 50mm) and different directional orientations (zero to twenty degrees from west-east direction). In general the behavior of edge wave propagation is more or less the same, except for the overflow behavior. For larger initial volume of water displaced (i.e. deeper water in the tsunami tank), more overflow and higher run-up height were observed. All wavelength, crest heights of and wave propagation speeds of the experiments are listed in Table 1. The wave speed, wave height and wavelength clearly increase with the amount of the water displaced. For all of the lab experiments, the run-up heights at the tombolo from north surges were larger than the ones from the south.

Table 1 Lab results of simulated (scaled down) tsunami run-up heights and wavelengths under different water depth conditions.

Water Depth (mm)	South side of tombolo Run up height (mm)	North side of tombolo Run up height (mm)	Wave Length (m)	Wave Height (mm)	Wave speed (m/sec) Measured at 2 m Away from water tank
30	18	28	0.3	8-9	0.9
40	21	30	0.45	14-15	1.13
50	23	33	0.5	20-22	1.18

6. CONCLUSIONS

These experimental simulations of edge waves along Phi-Phi Island using a physical hydraulic model had a good correlation with the field observations. The modeling simulations showed that edge waves were formed along the coastline of Phi-Phi Island. The formation and specific characteristics of the edge waves that were formed showed a dependence on water depths and initial directional orientation. The experimental observations helped explain that the damages on the tombolo of Phi-Phi Island were caused from surges from the north and not from the south. Also, the experiments showed

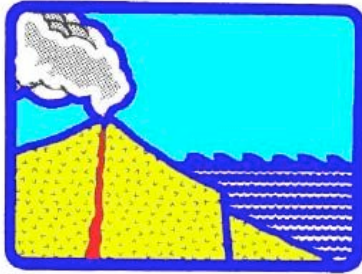
that areas of low elevation along the northern coastline of Phi-Phi Island became an outlet of tsunami surges, which also agrees with observations in the field. The high flow velocity of the tsunami is evident from the huge boulders that were carried on land by strong surges near the outlet. The results of the study provided a better understanding on the formation of edge waves and the potential impact that a tsunami in Hong Kong could have.

ACKNOWLEDGEMENT

The studies reported here were fully supported by The Hong Kong Polytechnic University through research Projects Nos. 87K1 and BBZF.

REFERENCES

- Bryant, E. (2001), *Tsunami: The underrated hazard*. Cambridge University Press, 320p.
- Dudley, W.C. and Lee M., (1998), *Tsunami! 2nd edition*, University of Hawaii Press, Honolulu, 386p.
- Komar, P.D., (1998), *Beach Processes and Sedimentation*. 2nd edition Prentice Hall, New Jersey.
- Wiegel, (1970). *Tsunamis*, Chapter 11, *Earthquake Engineering*, Prentice Hall, pp. 253-306.
- Soloviev, S.L. and Go, Ch. N., (1984), *A catalogue of tsunamis on the western shore of the Pacific Ocean (173-1968)*. Nauka Publishing House, Moscow, USSR, 310pp. Canadian Translation of Fisheries and Aquatic Sciences, 5077, 1984.
- Whalin, R.W. and Chatham, C.E., (1976), *Design of distorted harbor wave models*, *Proceedings of 15th Conference on Coastal Engineering*, American Society of Civil Engineering pp. 2103-2121.



SCIENCE OF TSUNAMI HAZARDS

International Journal of the Tsunami Society

Volume 29

Number 1

2010

DETERMINISTIC ANALYSIS OF THE TSUNAMI HAZARD IN CHINA

Yefei Ren¹, Ruizhi Wen², Baofeng Zhou³, Dacheng Shi⁴

^{1 3 4} Postgraduates, Dept. of Information Technology and Engineering Material, Institute of Engineering Mechanics, Harbin, China.

Email: renyefei@iem.net.cn, zbf166@126.com, shidc@iem.ac.cn

² Professor, Dept. of Information Technology and Engineering Material, Institute of Engineering Mechanics, Harbin, China.

Email: ruizhi@iem.net.cn

ABSTRACT

Seismic hazard analysis has reached a level of maturity in China. Such work has contributed significantly towards improvements of the national infrastructure in effecting programs of disaster preparedness and mitigation. However, the work on tsunami risk assessment is still in a preliminary stage. The present study proposes a deterministic method of tsunami hazard analysis based on coastal bathymetry and morphology, as well as on mathematical simulations, and evaluates the potential tsunami risk to China's coastal areas.

KEYWORDS: Earthquake; Tsunami; Hazard; Deterministic analysis method

1. INTRODUCTION

Presently, Probabilistic Seismic Hazard Analysis (PSHA) has been widely applied to seismic zonation and the evaluation of ground motions at specific sites. PDHA is necessary for normal seismic design of structures. The determination of ground motions is a key design factor for special construction projects, such as construction of nuclear power plants (Hu, 1988). Seismic hazard analysis has reached a level of maturity in China. It has provided needed technical support for urban planning and major engineering projects by giving technical references that can be used for vital policy decisions of the government in the establishment of the national system on disaster prevention and mitigation. However, no similar attention has been given to the analysis of the tsunami hazard. The importance of having such analysis performed, became evident after the catastrophic tsunami of December 26, 2004 in Sumatra and the Indian Ocean. The methodology on how to carry out work on tsunami hazard analysis in China is still a challenge. To help solve this problem, the present study provides and discusses a deterministic method of tsunami hazard analysis. First it delineates potential tsunami source regions that could affect China's coastline, based on historical earthquake and tsunami data, and sea bathymetry. Secondly, potential tsunami source regions are identified. Thirdly, based on numerical modeling, each tsunami source is evaluated and the potential coastal run-up heights are estimated. Finally, these wave heights are normalized and the extent of the tsunami hazard in China coastal areas is evaluated. Such methodology has been used in evaluating the tsunami hazard in the east coasts of Korea and Russia (Kurkin et al., 2004; Ho and Sung, 2001).

Research on tsunami hazard analysis begun in Japan and the United States of America in the 1980s. Japan's coast was divided into eight potential tsunami source regions (Rikitake and Aida, 1988). Based on the characteristic earthquake model, the annual exceeding probability of Japan assaulted by near-field tsunami was given. Annaka and Satake et al. (2007) used the logic-tree method to obtain the tsunami hazard curves (relationship between wave heights and annual exceeding probabilities) of Japan coast. Other scholars used a deterministic method based on numerical simulation, by assessing the hazards in coastal areas of Korea and Russia resulting from tsunamis generated along Japan's west coast (Kurkin and Pelinovskii et al., 2004; Ho and Sung, 2001). The tsunami hazards in the eastern Mediterranean region were evaluated through the use of historical tsunami database and by numerical simulation (Salamon and Rockwell et al., 2007). The probability of tsunami generation by landslides along southern California was evaluated by means of the Monte Carlo method (Watts, 2004). Also, GIS technology has being used in analyzing the tsunami hazard and in compiling tsunami hazard maps and flood inundation maps (Florence et al., 2005; Priest, 1995; Priest et al., 1997). Geist and Parsons (2006) applied the method of probabilistic tsunami hazard analysis in their work. Based on tsunami numerical simulation, the use of historical tsunami data and the Monte Carlo method separately, the tsunami hazard curves for Acapulco in Mexico and Cascadia on the U.S. West coast were evaluated. The studies pointed out two issues on the tsunami hazard analysis. The first issue is the difficulty on assigning specific earthquake probabilities to circum-Pacific subduction zones, and second issue is the limited amplitude range of tsunami measurements.

Research on tsunami hazard analysis in China begun in 1988, while Zhou Qinghai published a paper named “Tsunami Risk Analysis for China” in *Natural Hazards* (Zhou and Adams, 1988). In this paper, China tsunami historical database was used. By combining the geology and earthquake characteristics of China's continental shelf, the relative ratio of tsunami hazard in China coastal areas was evaluated. It suggested that the tsunami hazard ratio of Eastern Taiwan Coast, Continental Shelf and Bo Hai Bay is 16:4:1 and a zoning map of the tsunami hazard along China's coast was provided. Although the results were ambiguous, it was an important first step for tsunami research in China. After that there was a period of inactivity. However, after the 2004 Sumatra tsunami, the interest was revived. Limited to utilizing historical data, geology and geophysical characteristics of the continental shelf, the vulnerability of China coast to tsunamis was assessed (Wen and Ren, 2007; Yang, 2005; Yang and Wei, 2005). In 2007, Liu Yingchun, of the South China Sea Institute of Oceanology, (SCSIO, Chinese Academy of Sciences), used numerical modeling to analyze the probabilistic tsunami hazard for China's southeast coastal areas (Liu and Santos et al., 2007). Five major coastal cities of southeast China were specifically identified (Shantou, Xiamen, Xianggang, Aomen, and Tainan) as having probabilities of being struck by tsunami with amplitudes of 1-2m and above 2m separately. These results were more substantive and contributed to enhancing China tsunami research. In addition, Ren Yefei and Wen Ruizhi, scholars of IEM (Institute of Engineering Mechanics, China Earthquake Administration), following similarities with the seismic hazard analysis method, guidelines were provided (Ren, 2007) for a probabilistic tsunami hazard analysis, by suggesting the methodology on which this present work is based. Thus, this work can provide a theoretical basis and a technical reference for doing further research on tsunami hazard analysis in China.

2. DELINEATING POTENTIAL TSUNAMI SOURCE REGIONS

Tsunamis in the region are mostly generated by earthquakes with magnitudes above 6.5. There is no established recurrence frequency for tsunamigenic earthquakes in the Bohai and the Yellow Seas (Gao and Min, 1994), as there are in the East and South China Seas (Yang and Wei, 2005; Wei and Chen, 2005). In delineating potential tsunami sources that can affect China's coasts, regions of infrequent earthquakes are not included. Potential tsunami sources are selected along the Korean peninsula, the Sea of Japan, Ryukyu Islands, Taiwan and the Philippines. Plate tectonics, local geology, bathymetry, paleoseismological evidence, as well as historical earthquake and tsunami data, were the main parameters in delineating potentially tsunamigenic regions. Another criterion for selecting each source region was the depth of the sea, which must be deep enough to satisfy the condition for tsunami generation, generally believed to be more than 200m.

The historical database documents a total of 1470 significant earthquake events (listed by the Novosibirsk Tsunami Laboratory, in Russia), from 2150 B.C to 2002 A.D., in the area between 0°N to 45°N and 105°E to 150°E. (Figure 1). The historical database of the National Geophysical Data Center (U.S. NGDC), documents that 471 tsunami events occurred from 173 A.D. to 2007 A.D, between 0°N to 45°N and 105°E to 150°E. (Figure 2). By using global bathymetric data supplied by NGDC, the isobaths of China coast are drawn. The 200 m sea depth was selected as one of necessary conditions for tsunami generation, as shown in Figure 3. Based on such data, China potential tsunami

source regions were reasonably delineated, as shown in Figure 4.

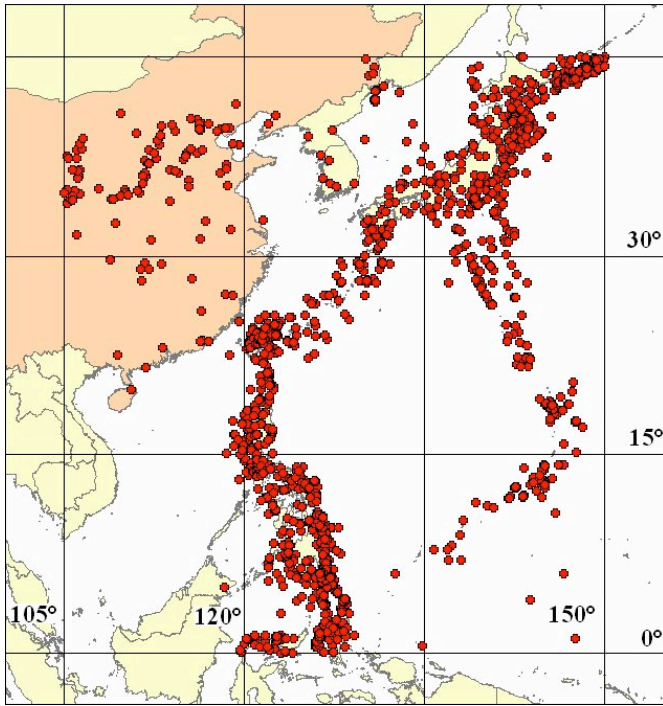


Fig. 1. Regional historical earthquakes

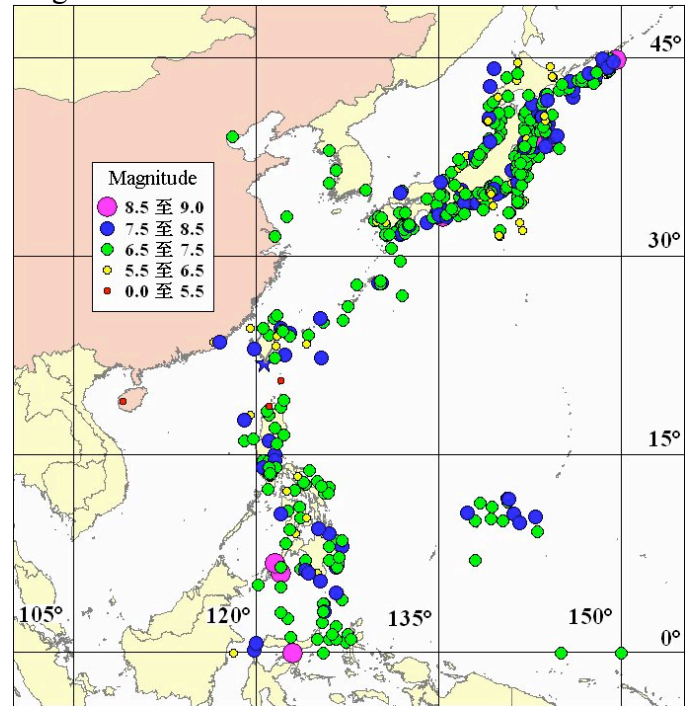


Fig. 2. Regional historical tsunami generation

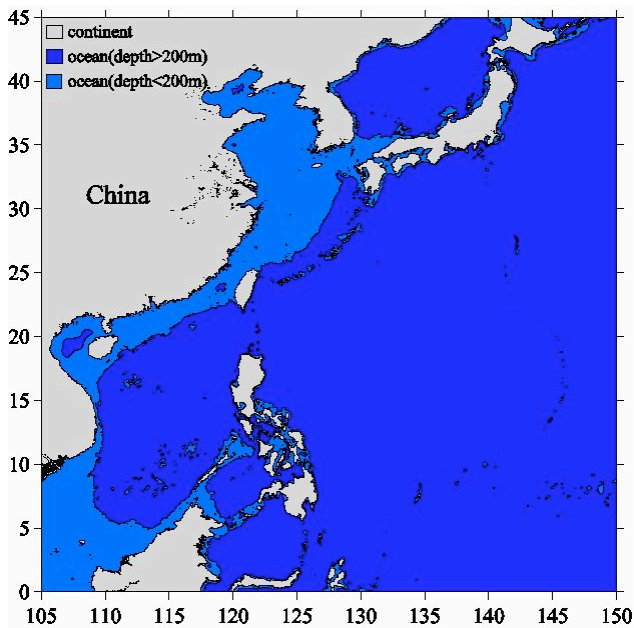


Fig. 3. Bathymetry of China coast (200m depth)

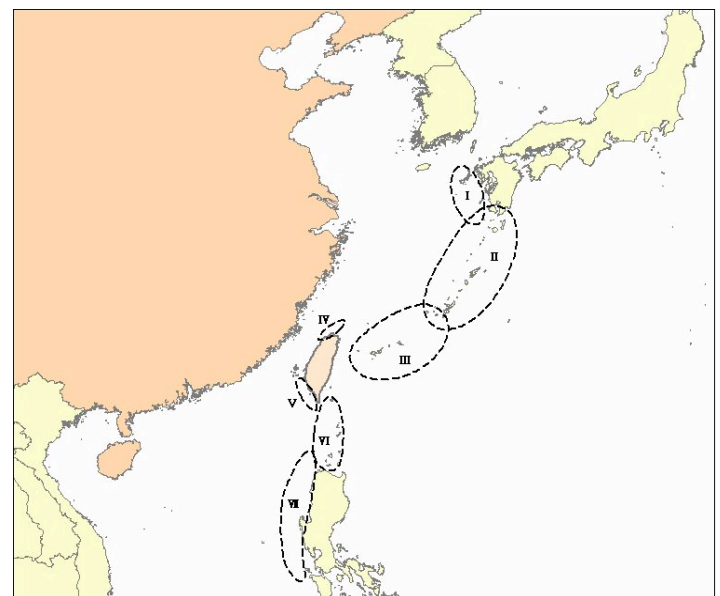


Fig. 4. Source regions of tsunamis that could potentially impact China's coasts.

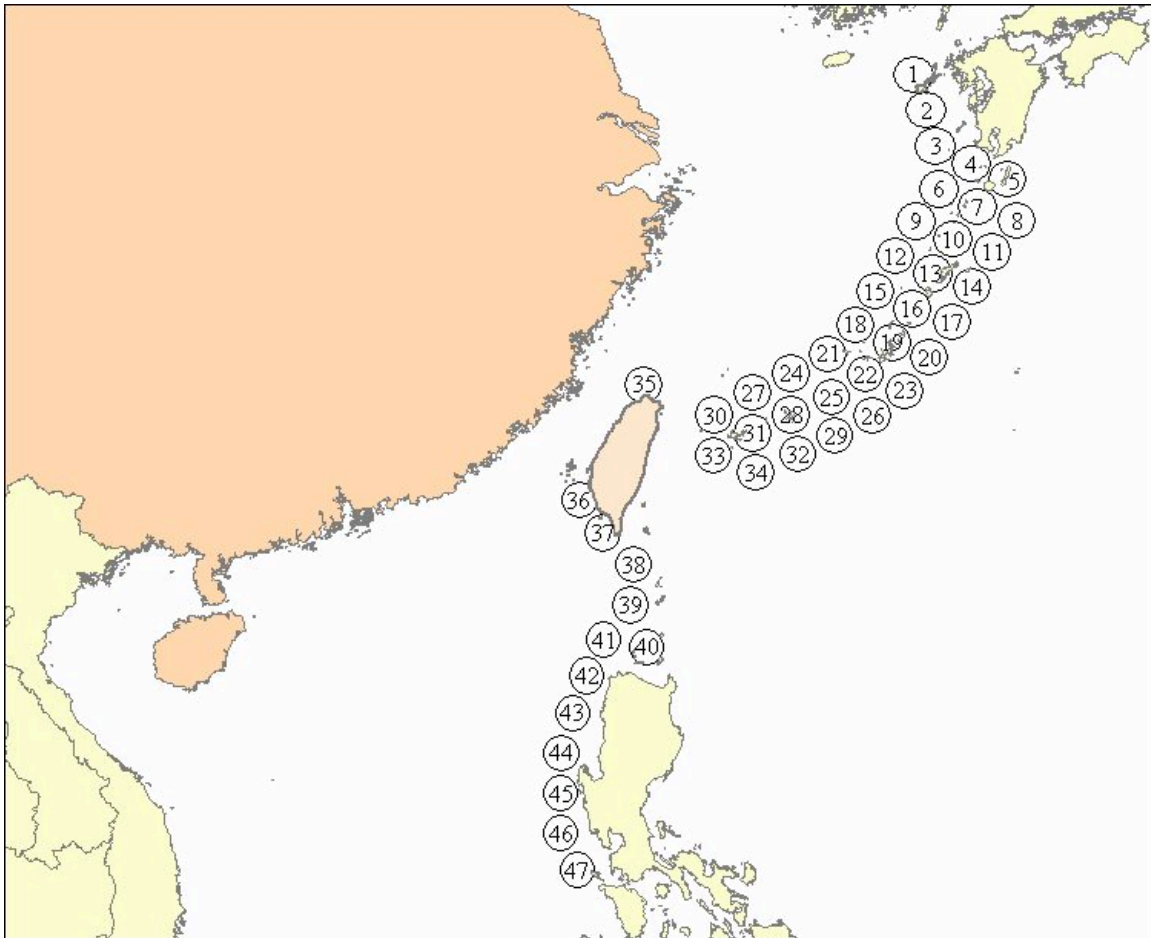


Fig. 5. Distribution of potential tsunami sources that can potentially impact China's coastlines.

3. DETERMINING POTENTIAL TSUNAMI SOURCES

For modeling purposes, 47 potential tsunami sources with 50km radius were selected, as shown in Figure 5 to apply initial water displacements. Each tsunami source was depicted as a cone-shaped area with maximum height of 5m, as shown in figure 6. It should be noted that the initial displacement field for each source in the numerical tsunami simulation was estimated on the basis of fault dislocation in elastic half-space. However, point sources were depicted due to the lack of fundamental information on active faults. Tsunami wave heights were normalized first, as not to result in erroneous assessment results that would unduly elevate the tsunami hazard along China's coasts.

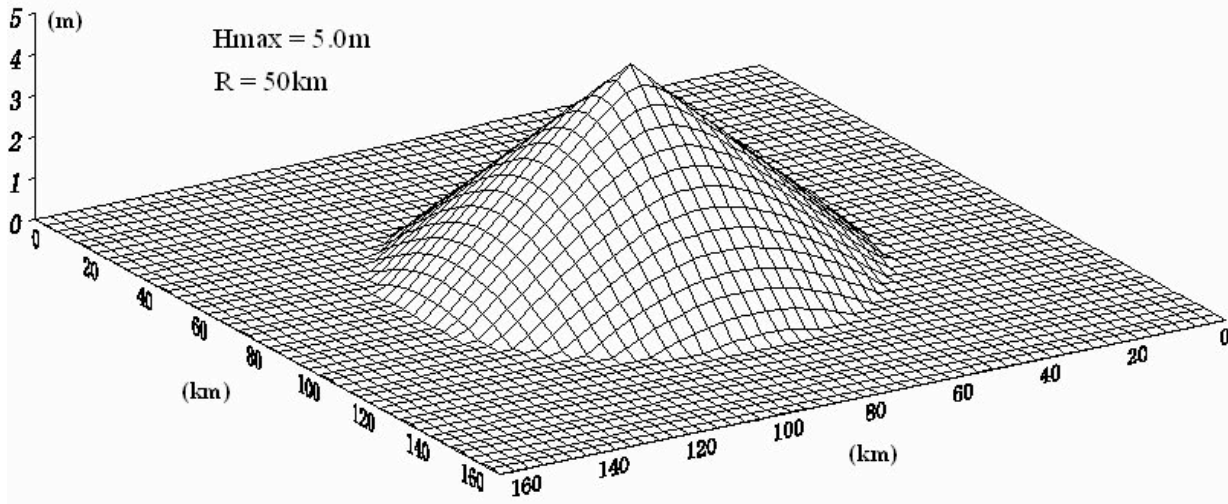


Fig. 6. The postulated shape of each potential tsunami source

4. MATHEMATIC CALCULATION

After the initial displacement fields were determined, waves were propagated from each tsunami source using a near-field tsunami numerical mode (Wai and Chau et al., 2005; Ren, 2007; Wen and Ren et al., 2007). The governing, nonlinear, shallow water equations were solved by means of finite difference methods.

$$\frac{\partial \eta}{\partial t} + \frac{\partial M}{\partial x} + \frac{\partial N}{\partial y} = 0 \quad (4.1)$$

$$\frac{\partial M}{\partial t} + \frac{\partial}{\partial x} \left(\frac{M^2}{D} \right) + \frac{\partial}{\partial y} \left(\frac{MN}{D} \right) + gD \frac{\partial \eta}{\partial x} + \tau_x D = 0 \quad (4.2)$$

$$\frac{\partial N}{\partial t} + \frac{\partial}{\partial x} \left(\frac{MN}{D} \right) + \frac{\partial}{\partial y} \left(\frac{N^2}{D} \right) + gD \frac{\partial \eta}{\partial y} + \tau_y D = 0 \quad (4.3)$$

Where, η is the vertical displacement of the water surface; $D = h + \eta$ is the total water depth; g is the gravity acceleration constant; $M = u(h + \eta)$ and $N = v(h + \eta)$ are the x and y-directional discharges, where u and v are the x and y-directional averaged particle velocities; τ_x and τ_y are the x and y-direction values of bottom frictions, which can be expressed by:

$$\tau_x = \frac{gn^2}{D^{10/3}} M \sqrt{M^2 + N^2}, \quad \tau_y = \frac{gn^2}{D^{10/3}} N \sqrt{M^2 + N^2} \quad (4.4)$$

Figure 7 below shows the tsunami heights along China's coasts resulting from the mathematical simulation of waves originating from the No.18 tsunami source. A maximum height of 2.67m occurred near the area with latitude 30°N., indicating that this was the region of the highest tsunami risk. Perhaps the high run-up value results from the short distance to the No.18 tsunami source.

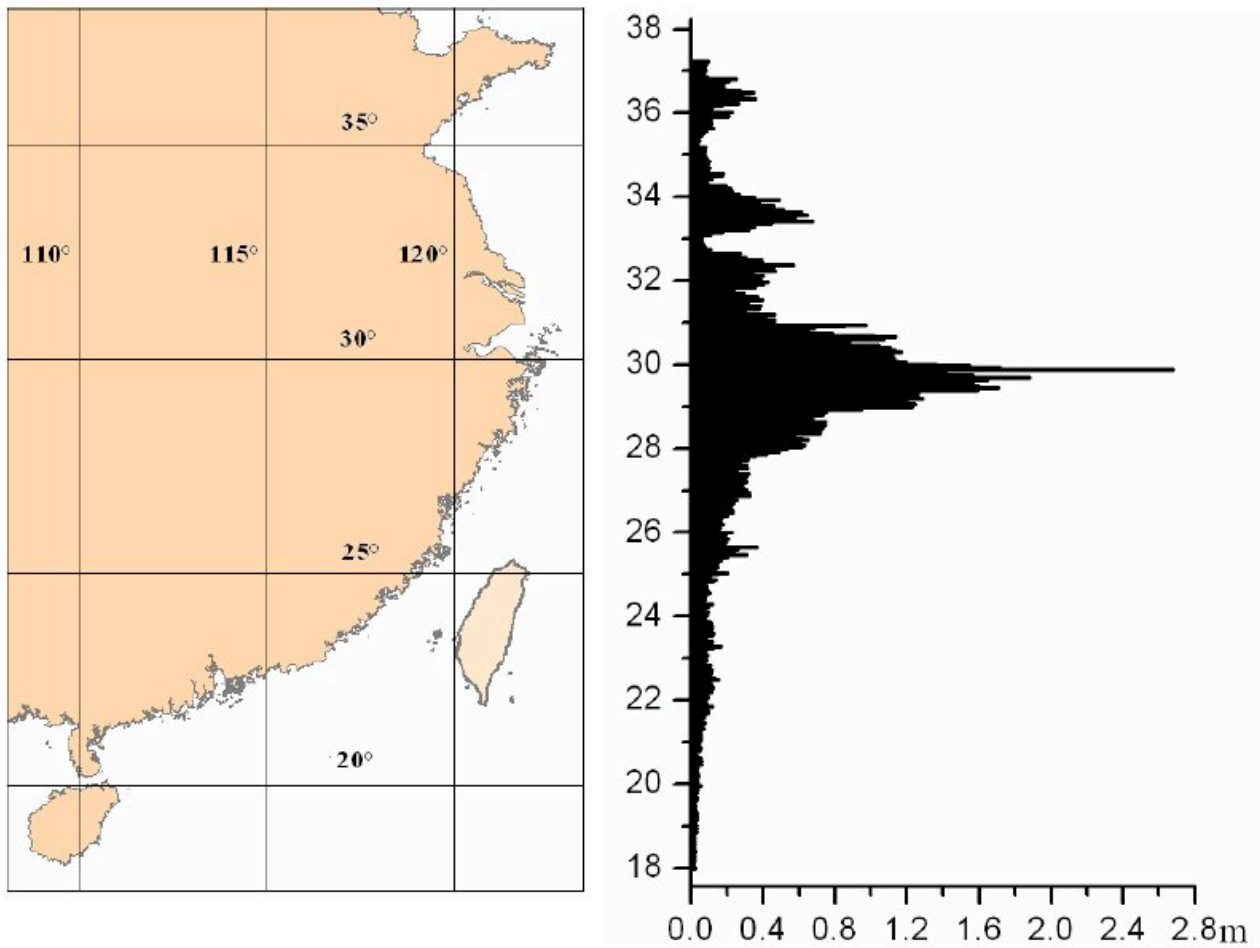


Fig. 7. Tsunami run-up heights along China coast from the No.18 tsunami source.

However, for a complete tsunami risk evaluation along China's coastlines, all the results from all potential sources must be comprehensively analyzed and integrated. Figure 8 summarizes the tsunami run-up heights from the mathematical modeling of all 47 potential sources.

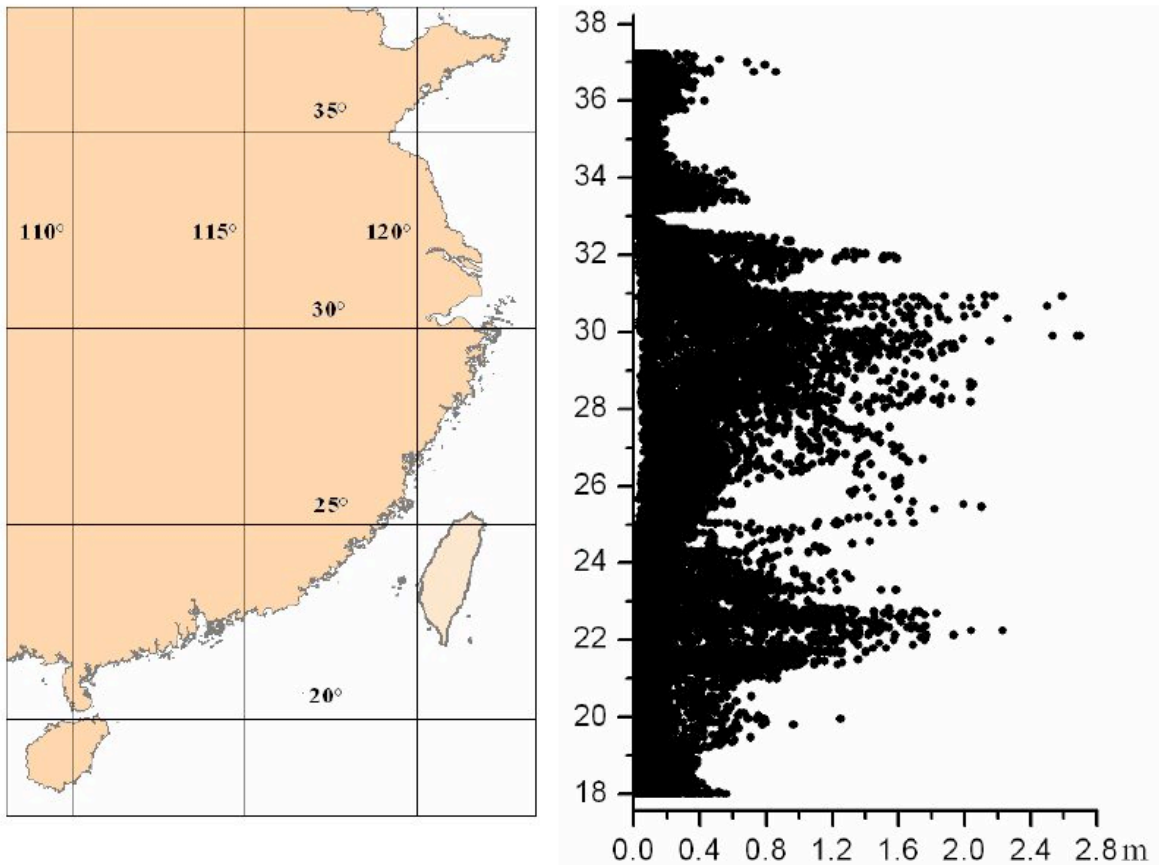


Fig. 8. Tsunami run-up heights along China's coast line from all 47 potential tsunami sources.

5. NORMALIZING TSUNAMI WAVE HEIGHTS

All tsunami wave heights were normalized by selecting from each group the maximum run-up heights. As a result, a series of ratios, which are less than 1, were obtained. Figure 9 shows the values resulting by the process of normalizing all tsunami run-up heights.

6. CONCLUSIONS

The tsunami run-up heights along China's coastlines will depend on earthquake parameters such as magnitude and type of faulting, as well as on the source's distance from the coast and coastal bathymetry and morphology, among other factors. In the present study, conical tsunami sources were used in order to eliminate the influence of some of the unknown earthquake source parameters such as magnitude and directionality due to faulting and angle of strike. All wave heights were normalized in order to eliminate the effects of that distance may have on tsunami propagation. As a result, the differences in the degree of tsunami hazard vulnerability along China's coastlines were determined primarily on the basis of coastal bathymetry and configuration. On the basis of such probabilistic tsunami hazard analysis as illustrated by Figure 9, it is concluded that:

1. The degree of tsunami hazard in Bohai Bay is considerably low, since it is a semi-enclosed basin that restricts the entry of tsunami energy from distant sources. Additionally, Bohai Bay does not have known sources that can generate tsunamis.

(2) From the Yellow Sea to Hainan Island and in three areas near the deltas of the Yangtze, Qiantang and Pearl river, the potential tsunami hazard is higher than in other coastal areas. On the basis of the proximity of earthquake sources, coastal areas along the East China Sea are more vulnerable, while coastal areas along the South China Sea are less vulnerable. The lowest tsunami hazard vulnerability is assigned to coastal areas fronting the Yellow Sea.

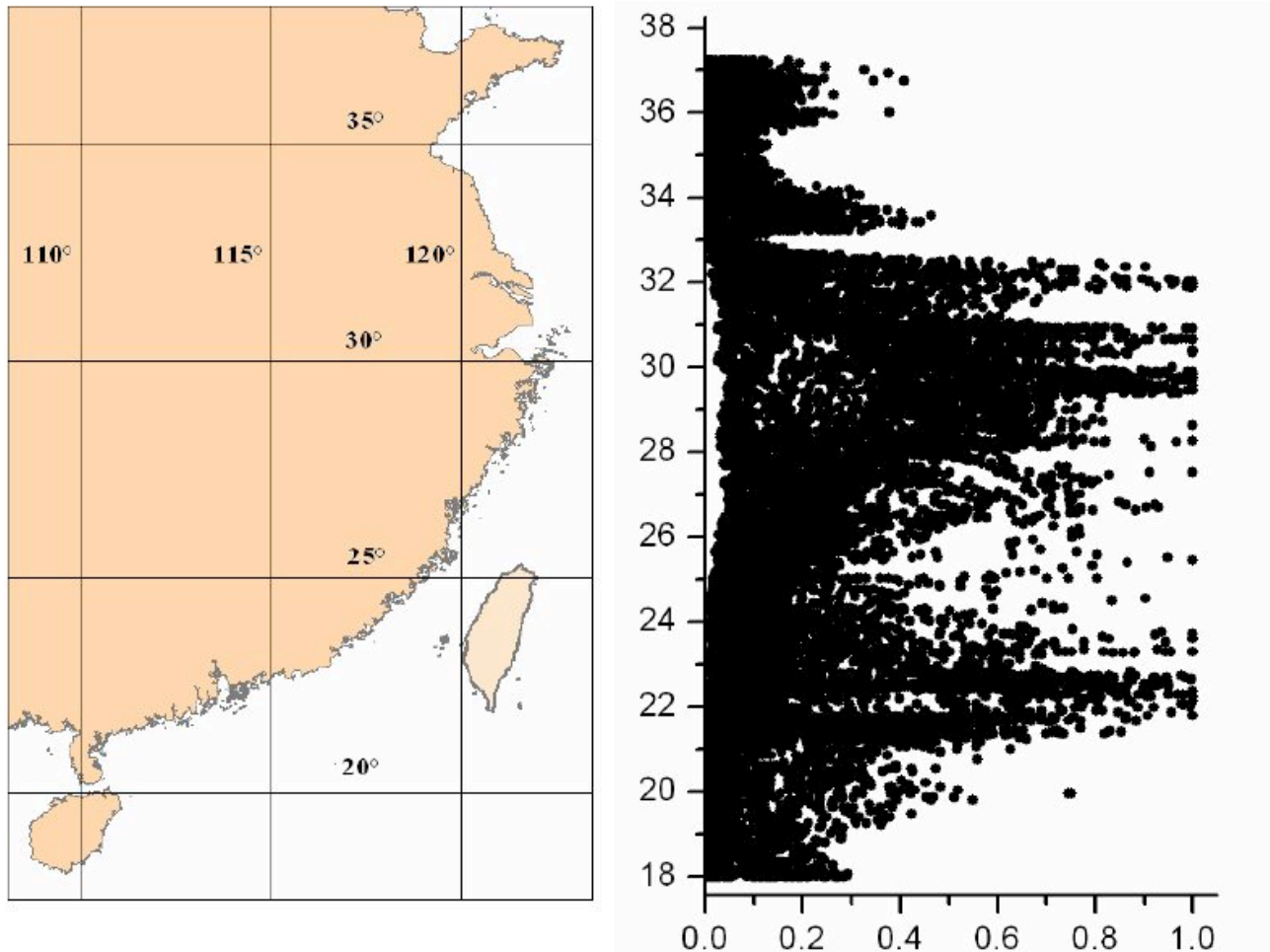


Figure 9. Values resulting from normalizing all tsunami run-up height.

ACKNOWLEDGEMENTS

The Joint Foundation of Seismic Sciences of China (A07080) supported this research.

Science of Tsunami Hazards, Vol. 29, No. 1, page 40 (2010)

REFERENCES

- Annaka, T., Satake, K., Sakakiyama, T. et al. (2007). Logic-tree Approach for Probabilistic Tsunami Hazard Analysis and its Applications to the Japanese Coasts. *Pure Appl. Geophys.*, 164, 577-592.
- Florence, L.W., Eric, L.G. and Angie, J.V. (2005). Probabilistic Tsunami Hazard Maps and GIS. 2005 ESRI International User Conference, San Diego, California, proceedings, 11pp.
- Gao, H. and Min, Q. (1994). Analysis on the possibility of tsunami generation in Bo Hai. *Marine Forecasts*, 11:1, 63-66 (in Chinese).
- Geist, E.L. and Parsons, T. (2006). Probabilistic Analysis of Tsunami Hazards. *Natural Hazards*, 37:3, 277-314.
- Ho, C. and Sung, J.H. (2001). Simulation of prognostic on the Korean coast. *Geophys. Res. Lett.*, 28:10, 2013-2016.
- Hu, Y. (1988). Earthquake Engineering, Seismological Publishing House, China.
- Kurkin, A.A., Pelinovskii, E.N., Choi, B.H. and Lee, J.S. (2004). A Comparative Estimation of the Tsunami Hazard for the Russian Coast of the Sea of Japan Based on Numerical Simulation. *Oceanology*, 44:2, 163-172.
- Liu, Y., Santos, A., Wang, S.M., Shi, Y., Liu, H., Yuen, D.A. (2007). Tsunami hazards along Chinese coast from potential earthquakes in South China Sea. *Phys. Earth Planet. Int.*, 163, 233-244.
- Priest, G.R. (1995). Explanation of mapping methods and use of the tsunami hazard maps of the Oregon coast. Oregon Department of Geology and Mineral Industries Open-file Report O-95-67.
- Priest, G.R., Myers III, E.P., Baptista, A.M., Fleuck, P., Wang, K., Kamphaus, R.A. and Peterson C.D. (1997). Cascadia Subduction Zone, Tsunamis-Hazard mapping at Yaquina Bay, Oregon. Oregon Department of Geology and Mineral Industries Open-File Report O-97-34, 144pp.
- Ren, Y. (2007). Study on China Earthquake Tsunami Hazard Analysis Based on Numerical Simulation: [Master's Degree Thesis]. Harbin: Institute of Engineering Mechanics, China Earthquake Administration, 135pp (in Chinese).
- Rikitake, T. and Aida, I. (1988). Tsunami hazard probability in Japan. *Bull. Seismol. Soc. Am.*, 78:3, 1268-1278.
- Salamon, A., Rockwell, T., Ward, S.N., Guidoboni, E. and Comastri, A. (2007). Tsunami Hazard Evaluation of the Eastern Mediterranean - Historical Analysis and Selected Modeling. *Bull. Seismol. Soc. Am.*, 97:3, 705-724.

Wai, O.W.H., Chau, K.T. et al. (2005). A preliminary numerical study of tsunami generated wave patterns in Hong Kong waters. 2005 Annual Meeting, Asian-Pacific Network of Centers for Earthquake Engineering Research, Jeju, South Korea, November 10-13.

Watts, P. (2004). Probabilistic predictions of landslide tsunamis off Southern California. *Marine Geology*, 203, 281-301.

Wei, B. and Chen, Y. (2005). Earthquake and tsunami. *South China Journal of Seismology*, 25:1, 43-49 (in Chinese).

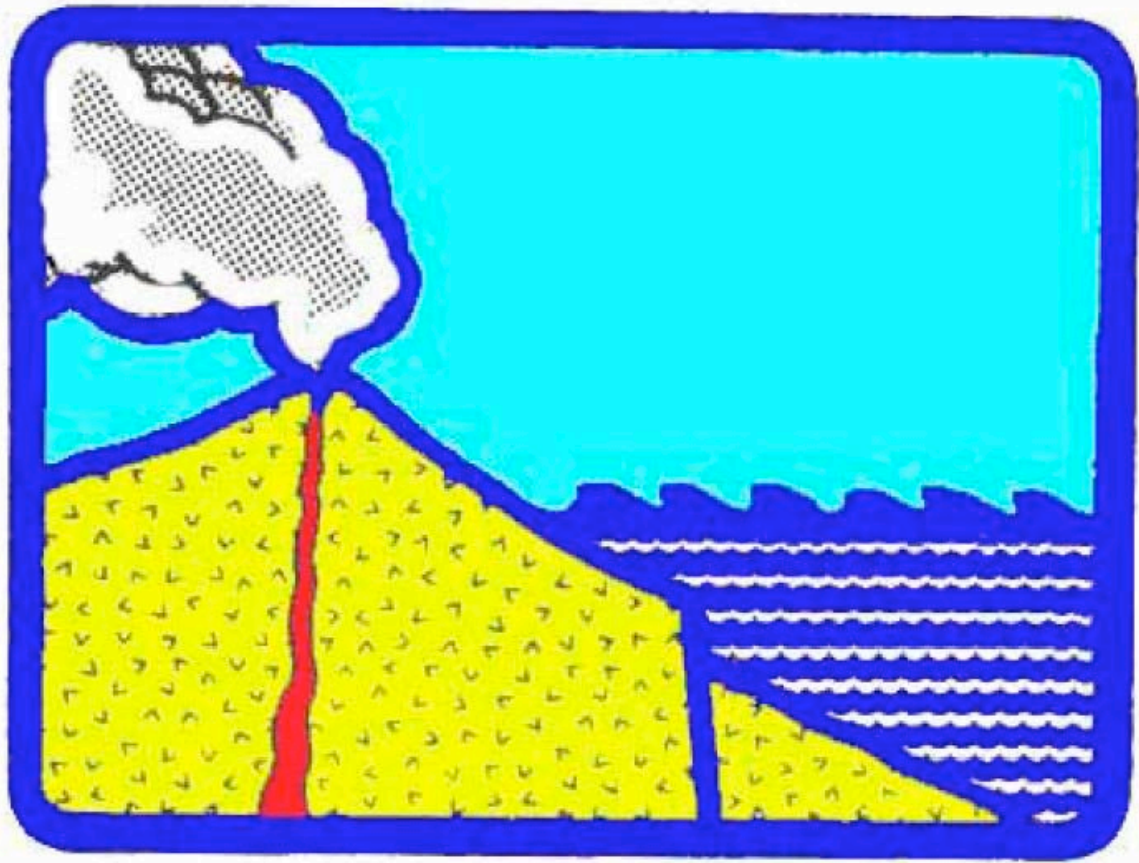
Wen, R. and Ren, Y. (2007). Preliminary study on tsunami hazard analysis in China. *World Earthquake Engineering*, 23:1, 6-11 (in Chinese).

Wen, R., Ren, Y., Zhou, Z. (2007). Preliminary study on numerical simulation of near-field tsunami. *Journal of Disaster Prevent and Mitigation Engineering*, Supplement, 447-450 (in Chinese).

Yang, M. (2005). The Risk Analysis of Seismic Tsunami and the Conception of the Warning System in Guangdong Province. *South China Journal of Seismology*, 25:4, 25-33 (in Chinese).

Yang, M. and Wei, B. (2005). The Potential Seismic Tsunami Risk in South China Sea and its Surrounding Region. *Journal of Catastrophology*, 20:3, 41-47 (in Chinese).

Zhou, Q. and Adams, W.M. (1988). Tsunami Risk Analysis for China. *Natural Hazards*, 1:2, 181-195.



Copyright © 2010

Tsunami Society International
1741 Ala Moana Blvd. #70
Honolulu, HI 96815, USA

WWW.TSUNAMISOCIETY.ORG